Chemistry 988 Lecture Notes

Nuclear Magnetic Resonance: Radiofrequency spectroscopy on nuclear spin states in a uniaxial constant magnetic field

$$\mathbf{B} = B_0\check{\mathbf{z}} \qquad \text{(I.1.1)}$$

B_0 is on the order of 1-20 T

The rf frequencies vary between 1 and 1000 MHz.

Advantages:

Control over Timing, Pulse Length

Prelude: Short History of NMR

A. Understanding of Magnetism – Late 19th century
B. Discovery of Spin – 1920's
C. WWII – Development of RF technology
D. First Observation of NMR Signal in paraffin:
    1. E. M. Purcell, H. C. Torrey, and R. V. Pound, *Physical Review*, **69**, 37 (1946)
    2. F. Bloch, W. W. Hansen, and M. Packard, *Physical Review*, **69**, 127 (1946)
    3. Nobel Prize in Physics - 1952
E. Discovery of Chemical Shift (1949)
F. First Commercial NMR Spectrometer – 1953 (Varian)
G. 50's and 60's: Spin Echoes, Nuclear Overhauser Effect, ENDOR, Magic Angle Spinning
H. Fourier Transform NMR: R. R. Ernst and W. A. Anderson, *Rev. Sci. Instruments*, **37**, 93 (1966) – Nobel Prize in Chemistry 1992
I. 70's:
    1. 2D NMR:
        a. J. Jeener – 1971
        b. W. P. Aue, E. Bartholdi, and R. R. Ernst, *J. Chem. Phys.*, **64**, 2229 (1976).
    2. Cross Polarization: A. Pines, M. G. Gibby, J. S. Waugh, *J. Chem. Phys.*, **59**, 569 (1973).
J. 80's
    1. Magnetic Resonance Imaging (Paul Lauterbur – University of Illinois)
    2. Protein Structure Determination in Liquids (K. Wuthrich, A. Bax)
H. 90's: Protein Structure Determination in Solids?

Harris, Chapter 1

Section 1-2: Quantization of Angular Momentum

Nuclear Spin is a form of angular momentum. Classically, angular momentum is:

$$\mathbf{P} = \mathbf{r} \times \mathbf{p} = \mathbf{r} \times m\mathbf{v} \qquad \text{(I.2.1)}$$

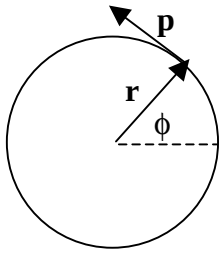

The angular momentum vector is perpendicular to the page.

Angular momentum is always quantized, that is it has discrete values. This is only of consequence when it has small values, as it does in nuclei, atoms, and molecules. The quantization equation for the squared magnitude of angular momentum is:

$$P^2 = \hbar^2[R(R+1)] \qquad \text{(I.2.2)}$$

where R is an integer. Angular momentum is a vector. Its value is defined or quantized along only one spatial axis and is not defined along the other spatial axes. (Show Figure 1-1) For magnetic resonance, this axis is typically the direction of the external magnetic field. We typically label this as the z axis and have:

$$P_z = \hbar m_R \qquad \text{(I.2.3)}$$

where

$$m_R = R, R-1, R-2, \ldots, -R \qquad \text{(I.2.4)}$$

P_x and P_y do not have definite values. Note that for R>0 (necessary for observation of NMR signals):

$$P^2 > P_z^2 \qquad \text{(I.2.5)}$$

There is uncertainty in the determination of ϕ, P_x, and P_y.

Section 1-3: Electron and Nuclear Spin

The existence of electron and nuclear spin angular momentum was inferred from atomic physics experiments in magnetic fields and from relativistic quantum mechanical theory. In atoms and molecules to a good approximation, spin angular momentum is not coupled to spatial angular momenta such as orbital motion of electrons or rotational motion of molecules. There are however small fine and hyperfine couplings between spin and spatial angular momenta which are observable in highly resolved atomic and molecular spectra.

We tend to think classically about angular momentum like in the first figure. The word 'spin' confuses us because we think of the planetary model for the atom with the nucleus and electrons spinning about their respective axes. It is best to think of spin as another angular momentum associated with the electron or nucleus but not associated with spinning motion.

The I (R) value for the electron, proton, and neutron are all ½. For nuclei composed of multiple protons and neutrons, the following even/odd general rules apply

Mass Number	Charge	I	Examples
Odd	Odd or Even	Half-Integer	^{13}C, ^{15}N, ^{29}Si (I=1/2), ^{27}Al (I=3/2)
Even	Even	Zero	^{12}C, ^{16}O, ^{32}S
Even	Odd	Integer	^{2}H, ^{14}N (I=1), ^{10}B (I=3)

Section 1-4: Nuclear Magnetic Moments

For electrons and nuclei with non-zero spin, there is an associated *magnetic dipole moment*. The spin angular momentum and magnetic dipolar moments are *proportional* and *colinear*. So, importantly for magnetic resonance, the z components of the spin angular momentum and magnetic dipole moments are proportional and colinear.

First of all, what is a magnetic dipole moment?

Remember that classically, magnetism arises from electric currents (motion of charge).

We wish to approximate the magnetic potential and field (analogous respectively to the electric voltage and electric field) far from the electric currents. See David J. Griffiths, *Introduction to Electrodynamics*, Chapter 5 as a good reference.

The magnetic vector potential for a loop of constant current I at point P is:

$$\mathbf{A}(C) = I\int(1/\rho)d\mathbf{l} \qquad (I.4.1)$$

This is a contour integral around the loop using d**l**.

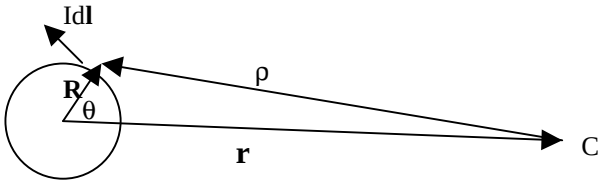

The magnetic field **B**(C) is found by:

$$\mathbf{B}(C) = \nabla \times \mathbf{A}(C) \qquad \text{(I.4.2)}$$

$$\nabla = (\partial/\partial x)\mathbf{x} + (\partial/\partial y)\hat{\mathbf{y}} + (\partial/\partial z)\check{\mathbf{z}}$$

∇ represents the gradient (slope) of **A**. X represents the cross product. The magnetic field is perpendicular to the potential.

When R << r, we can approximate

$$1/\rho = (1/r)\Sigma_{n=0}^{\infty} (R/r)^n P_n(\cos\theta) \qquad \text{(I.4.3)}$$

where $P_n(\cos\theta)$ is the Legendre polynomial

$$\begin{aligned} P_0(\cos\theta) &= 1 \\ P_1(\cos\theta) &= \cos\theta \\ P_2(\cos\theta) &= \tfrac{1}{2}(3\cos^2\theta - 1) \end{aligned} \qquad \text{(I.4.4)}$$

We expand **A**(C) in inverse powers of R/r (already a small number for R << r) and only keep the lowest order terms. When we expand the magnetic vector potential using Eq. (I.4.3),

$$\mathbf{A}(C) = I(1/r)\int d\mathbf{l} \;+\; I(1/r)^2 \int R\cos\theta \, d\mathbf{l} \;+\; \ldots. \qquad \text{(I.4.5)}$$

The first term represents the magnetic monopole potential and is always zero for a closed loop. The second term represents the magnetic dipole potential and can written as:

$$\mathbf{A}_{dip}(C) = (\mu \times \mathbf{r})/r^3 \qquad \text{(I.4.6)}$$

where **r** is the vector from the center of the loop to point C and and μ is the dipole moment represented by the equation

$$\mu = I \int R\cos\theta \, d\mathbf{l} = (I/2) \int \mathbf{R} \times d\mathbf{l} \qquad \text{(I.4.7)}$$

For a flat current loop, $\mu = I\mathbf{a}$ where a is the area of the loop and the vector is normal to the plane of the loop. Note that the dipole moment is a vector, that is it has definite **x,y,z** spatial components.

One can use Eqs. (I.4.2) and (I.4.6) to derive the magnetic dipolar field

$$\mathbf{B}_{dip}(C) = 3(\mu \cdot \mathbf{r})\mathbf{r}/r^5 - \mu/r^3 \qquad (I.4.8)$$

The field drops off with distance as r^3 and is the sum of two vector components. One component is parallel to the dipole moment vector μ and one component is parallel to the **r** vector. (Show Griffiths picture).

So a magnetic dipole moment really corresponds to a particular kind of magnetic field. For NMR, this field is associated with the nucleus of interest.

Now that we understand the magnetic dipole moment, the next question is: Why should the magnetic dipole moment be proportional and colinear with the spin angular momentum? We try to understand this with a classical model of orbital angular momentum and magnetic moments, the Bohr atom.

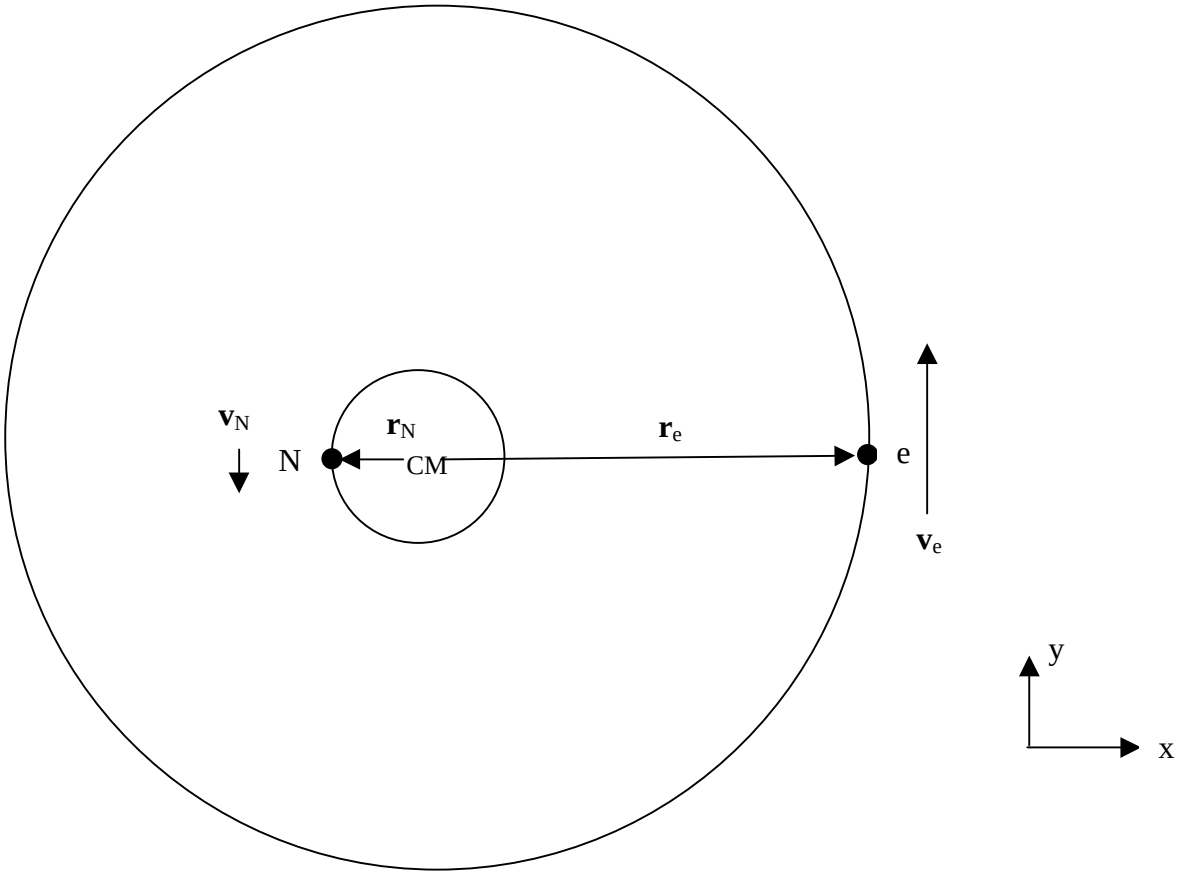

The nucleus and electron orbit with circular motion in the xy plane about their center of mass (CM). The ratio $r_N/r_e = m_e/m_N$ which is ~ 1/2000 for a proton nucleus.

Consider the electron first. It has angular momentum

$$\mathbf{P}_e = \mathbf{r}_e \text{ X } \mathbf{p}_e = \mathbf{r}_e \text{ X } m_e\mathbf{v}_e = m_e\mathbf{r}_e \text{ X } (2\pi r_e/T_e)\mathbf{v}_e = m_e r_e^2 \omega_e \check{\mathbf{z}} \quad \text{(I.4.9)}$$

where T_e is the orbit period and $\omega_e = 2\pi/T_e$ is the angular velocity. Note that the $\mathbf{v}_e$ in the third expression is unitless. I don't have a way to show this easily on the computer.

Now derive the dipole moment of the loop. Because of the negative electronic charge, the current is in the opposite direction to the electronic orbital motion.

$$\mathbf{I}_e = -e/T_e\mathbf{v}_e = (-e\omega_e/2\pi)\mathbf{v}_e \quad \text{(I.4.10)}$$

where e is the electronic charge. The magnetic moment associated with this current is:

$$\mu_e = I_e A_e \check{\mathbf{z}} = (-e\omega_e/2\pi)(\pi r_e^2)\check{\mathbf{z}} = -(e\omega_e r_e^2/2)\check{\mathbf{z}} \quad \text{(I.4.11)}$$

So, combining Eqs. (I.4.9) and (I.4.11),

$$\mu_e = (-e/2m_e)\mathbf{P}_e \quad \text{(I.4.12)}$$

So, the electronic orbital angular momentum and associated magnetic dipole moment are antiparallel. As angular momentum is quantized as $\hbar I(I+1)$, the electron magnetic moment will be quantized in units of $e\hbar/2m_e = 9.27410 \text{ x } 10^{-24}$ J/T. This unit is known as μ_B, the *Bohr magneton*. A similar derivation can be done for the nucleus which gives

$$\mu = (Ze/2m_N)\mathbf{P} \quad \text{(I.4.13)}$$

where Z is the charge of the nucleus. The *nuclear magneton* μ_N is defined for a proton nucleus and is $5.05095 \text{ x } 10^{-27}$ J/T. Note that nuclear magnetic moments are typically three orders of magnitude smaller than electron magnetic moments.

The point of this derivation is to demonstrate that there is a colinear, proportional magnetic dipole moment associated with angular momentum of a charged particle. The coefficients of proportionality between electron or nuclear spin magnetic moments and their respective magnetic moments are close to but not quite equal to the factors in I.4.12 and I.4.13, respectively. The *electron g* and *nuclear* g_N factors are multiplicative factors in the following general equations for the electron and nuclear spin magnetic moments:

$$\mu_e = -g\mu_B\mathbf{P}_e/\hbar \quad \text{(I.4.14)}$$

$$\mu = g_N\mu_N\mathbf{P}/\hbar \quad \text{(I.4.15)}$$

The electron g factor is 2.0023 and can be calculated from quantum electrodynamics. The nuclear g_N factor is specific to a given nucleus and varies between ~ -5 and +5. The proton g_N

factor is 4.83724. Eq. (I.4.15) can also be expressed in terms of the *gyromagnetic ratio* γ defined by:

$$\gamma = g_N \mu_{\underline{N}} / \hbar \qquad \text{(I.4.16)}$$

so that

$$\mu = \gamma \mathbf{P} \qquad \text{(I.4.17)}$$

Since the magnitude of P is $\hbar[I(I+1)]^{1/2}$, the scalar version of Eq. (I.4.17) is

$$\mu = \gamma \hbar [I(I+1)]^{1/2} \qquad \text{(I.4.18)}$$

Unfortunately, there appears to be no consistent way for expressing g_N and γ factors. For example, in Tables 1 and 2 in the back of Harris, they actually include the factor $[I(I+1)]^{1/2}$ in these tables. The CRC uses a different standard and includes a factor of I instead.

Section 1-5: Nuclei in a Magnetic Field

In the absence of a magnetic field, (Show Fig. 1-2), the m_I levels are degenerate, that is they have the same energy. In the presence of a magnetic field, their levels are split by the interaction

$$U = -\mu \cdot B \qquad \text{(I.5.1)}$$

This can be derived from classical electrodynamics and is intuitive if you've ever played with small bar magnets. These magnets want to align in one direction but not in the other. In the presence of a uniaxial field of constant magnitude $\mathbf{B}_0 = B_0 \check{\mathbf{z}}$, the nuclear spin angular momentum is quantized along z so that:

$$U = -\mu_z B_0 = -\gamma P_z B_0 = -\gamma \hbar m_I B_0 \qquad \text{(I.5.2)}$$

The selection rule for magnetic dipole transitions is $\Delta m_I = \pm 1$. For positive γ, the energy increases as m_I decreases. Resonant absorption will take place with radiation of energy

$$\Delta U_{abs} = |\gamma \hbar B_0| \qquad \text{(I.5.3)}$$

This corresponds to resonant frequency $\gamma B_0 / 2\pi$. So, the NMR frequency is proportional to both γ and B_0. For a 9.4 T magnet using the γ factor from Harris appendix 1, the resonant frequency for ^{1}H is:

$$\nu = [(4.83724)/(0.5 * 1.5)^{1/2}](5.05095 \times 10^{-27} \text{ J/T})(9.4 \text{ T})/(6.626 * 10^{-34} \text{ J-sec}) \qquad \text{(I.5.4)}$$
$$= 400.24 \text{ MHz}$$

Nuclei with $I \geq 1$ also have an *electric quadrupole moment* (draw picture of monopole, dipole, quadrupole) in addition to their magnetic dipole moment. The electric quadrupole moment

makes an important contribution to the NMR spectrum. The exact expression for the electric quadrupole moment can be derived in a means similar to Eqs. (I.4.1-I.4.8). In this case, we are trying to approximate the electric potential (voltage) of the nucleus. In the derivation, we use the electric potential V(C) instead of the magnetic potential **A**(C). The electric field is derived from the gradient of the potential: $\mathbf{E}(C) = \nabla V(C)$.

Dipoles interact with *fields* while *quadrupoles* interact with *field gradients* or the derivative of the field with respect to position. In particular, the nuclear electric quadrupole interacts with the *electric field gradient at the nucleus.* This field gradient is determined by the electronic environment at the nucleus which is in turn determined by the chemical bonding of the nucleus.

Even in the absence of an external magnetic field, the nuclear spin states are quantized by the quadrupole/electric field gradient interaction, that is different values of m_I have different quadrupolar energies. Transitions between these m_I states can be observed in the absence of an external magnetic field by pure *nuclear quadrupole resonance*.

In the presence of the external magnetic field, the quantization and energy levels of the m_I states are complex and depend on the relative strengths and orientations of the magnetic dipole/external magnetic field and electric quadrupole/electric field gradient interactions.

In both liquids and solids, NMR spectra of quadrupolar nuclei are usually broader than those of spin ½ nuclei. Quadrupolar nuclei also relax more quickly than spin ½ nuclei because of the larger fluctations in the electric field gradient relative to local magnetic fields.

Section 1-6: Larmor Precession

This section contains a model which provides a different insight into magnetic resonance. The model is a mix of classical and quantum mechanics. The quantum mechanical input is to consider the magnetic dipole moment as being tilted with respect to the external magnetic field with angle $\theta = \cos^{-1}\{m_I/[I(I+1)^{1/2}\}$. Classically, the external magnetic field will exert a torque **N** on the magnetic dipole which results in precessional motion of the dipole about the external magnetic field (Fig 1-4). This can be derived from:

$$\mathbf{N} = \mu \text{ X } \mathbf{B}_0 \qquad \text{(I.6.1)}$$

This torque is perpendicular to both μ and $\mathbf{B}_0$. We use relationships between torque, angular momentum, and magnetic moment to derive:

$$\mathbf{N} = d\mathbf{P}/dt = (1/\gamma)d\mu/dt = \mu \text{ X } \mathbf{B}_0 \qquad \text{(I.6.2)}$$

$$d\mu/dt = \gamma\mu \text{ X } \mathbf{B}_0 = \mu \text{ X } \gamma B_0\mathbf{z} = \gamma B_0(\mu \text{ X } \mathbf{z}) \qquad \text{(I.6.3)}$$

$$d\mu/dt = -\omega_i(\mathbf{z} \text{ X } \mu) \qquad \text{(I.6.4)}$$

So, the dipole moment precesses about the external magnetic field with Larmor frequency $\nu_i = -\omega_i/2\pi$. For positive γ and B_0, the precession is counterclockwise.

Absorption or emission of radiative energy at the Larmor frequency will cause the dipole moment vector to change its direction relative to **z**, that is to change its m_I state (Show Fig. 1-6). To understand this, remember that electromagnetic radiation consists of a traveling wave with orthogonal transverse electric and magnetic fields. These fields oscillate in both time and space (show picture). For radiation polarized along the **x** axis, the oscillating magnetic field can be expressed as:

$$\mathbf{B}_1(t) = B_1\cos[2\pi(x/\lambda - \nu t) + \delta]\mathbf{x} \qquad \text{(I.6.5)}$$

where λ is the wavelength and ν is the frequency of the radiation and δ is some constant phase. This expression can be decomposed as the sum of two components, one of which rotates clockwise around the **ž** axis and one of which rotates counterclockwise about the **ž** axis.

$$\mathbf{B}_1(t) = B_1/2\{\cos[2\pi(x/\lambda - \nu t) + \delta]\mathbf{x} + \sin[2\pi(x/\lambda - \nu t) + \delta]\mathbf{y}\}$$

$$+ B_1/2\{\cos[2\pi(x/\lambda - \nu t) + \delta]\mathbf{x} - \sin[2\pi(x/\lambda - \nu t) + \delta]\mathbf{y}\} \qquad \text{(I.6.6)}$$

If $\nu = \nu_i$, the latter field will rotate synchronously with the magnetic moment μ and can have some consistent effect on the angle between μ and **z**. For example if δ is set such that the resonant rotating field is 90° ahead of μ, then the B_1 field will exert a constant torque which increases the θ angle between μ and **z**. To see this, Eq. (I.6.4) can be rewritten to include the effect of $\mathbf{B}_1$:

$$d\mu/dt = -\omega_i(\mathbf{z} \times \mu) - (B_1/2)(\mathbf{x} \times \mu) \qquad \text{(I.6.7)}$$

This equation is written in the *rotating frame* where the **x** and **y** axes rotate about **z** at the Larmor frequency. The first term gives the Larmor precession of μ about the external magnetic field while the second term increases θ and changes m_I (Show picture).

Section 1-7: The Intensity of an NMR Signal

We consider the various effects which go into the intensity of an NMR signal. We consider the I = ½ system with two states, m_I = ½ and m_I = -½. The RF absorption intensity is the sum of signals from the individual spins in the system. If there are equal numbers of spin up and spin down nuclei, the net RF absorption will be zero because equal numbers of RF photons will be absorbed and emitted.

So, the rate of total energy absorption R will be proportional to:

(1) the population difference between the m_I = ½ and m_I = -½ states.
(2) the probability of inducing a transition between these states
(3) the energy absorbed or emitted in a transition

These factors are proportional to:

(1) $N\Delta U/2kT = N\gamma\hbar B_0/2kT$

where N is the number of nuclei in the sample, ΔU is the energy difference between the $m_I = ½$ and $m_I = -½$ states, k is Boltzmann's constant, and T is the temperature. Eq. (I.5.3) was used to calculate ΔU. (Problem 1-15).

(2) $(\gamma B_1)^2$

This is calculated from the quantum mechanical derivation for transition probabilities (Fermi's Golden Rule) – see P. W. Atkins, Molecular Quantum Mechanics or some similar advanced quantum mechanics textbook. The transition probability is proportional to the square of the interaction which causes the transition. In our case, this interaction is $-\mu \cdot \mathbf{B}_1$. The square of this interaction is proportional to $(\gamma B_1)^2$.

(3) $\gamma\hbar B_0$ – from Eq. (I.5.3)

So, taking the product of (1), (2), and (3) and only including factors which vary with the spectrometer and sample conditions, the rate of RF energy absorption is:

$$R \propto N\gamma^4 B_1^2 B_0^2/T \qquad \text{(I.7.1)}$$

The total signal intensity S is proportional to R/B_1:

$$S \propto N\gamma^4 B_1 B_0^2/T \qquad \text{(I.7.2)}$$

In real spectra, the signals have some linewidth $\Delta\nu$ which may vary with temperature, B_0, or γ (choice of nucleus.) Often, we are interested in the intensity at the resonant frequency ν_0 . This is:

$$S(\nu_0) \propto S/\Delta\nu \propto N\gamma^4 B_1 B_0^2/T(\Delta\nu) \qquad \text{(I.7.3)}$$

Let's compare relative sensitivity of NMR spectra under various conditions. We will arbitrarily assign as 1.0000 the sensitivity of ^{1}H at B_0 = 7.05 T (300 MHz ^{1}H Larmor frequency). We also calculate the signal-averaging time $T_{s.}$required to obtain the equivalent signal-to-noise ratio. This is proportional to the inverse square of the sensitivity because $S/N \propto (\text{number of scans})^{1/2}$. For example, if one removes half of the sample, one loses half of the signal and has to signal average for four times longer to obtain the S/N one had initally with the full sample.

Nucleus	N (Percent Abundance)	B_0 (T)	T (K)	$\Delta\nu$ (Hz)	$S(\nu_0)$ (relative)	$T_{s.a.}$ (rel.)
^{1}H (liquid)	100	7.05	300	10	1.000000	1 min.
^{1}H (liquid)	100	14.10	300	10	4.000000	1 sec.
^{13}C (liquid)	1 (nat.ab.)	7.05	300	5	0.000078	300 years
^{13}C (solid)	100 (enriched)	9.40	220	100	0.000947	2 years

If one only considers sensitivity, it is optimal to detect ^{1}H at as high field as possible. Of course, the point of NMR is to obtain information about a particular chemical system and their may be greater information content in other nuclei such as ^{13}C, ^{15}N, ^{29}Si, ^{27}Al, ^{11}B, ^{23}Na, etc. Isotopic enrichment may be necessary for nuclei other than ^{1}H, and one usually needs more material for these lower γ nuclei.

Magnetic field strength is dictated by current technology and money. For example, a 300 MHz liquids spectrometer is ~ $200,000 while a 600 MHz liquids spectrometer is ~ $800,000. It is not currently possible to obtain a commercial NMR magnet with field strength greater than about 20 T.

In addition to these fundamental factors which affect sensitivity, there are also instrumental factors. The 'efficiency' of the NMR probe (Draw picture of NMR tuning) determines the B_1 field strength and noise is determined by the RF detection electronics.

Section 1.8 Electronic Shielding

The actual magnetic field experienced by the nucleus is *different* than the external field because of the magnetic fields of the electrons. These electronic fields are the results of electronic currents *induced* by the external magnetic field. Calculation of the actual induced currents is complicated(See Slichter, Chapter 4) so we try, as usual, to understand with a simple example. We consider the *cyclotron* motion of the electrons about the external magnetic field direction (See Figure 1-7 (a)). This is circular motion of the electrons about the external magnetic field direction. The circle does not have to contain the nucleus.

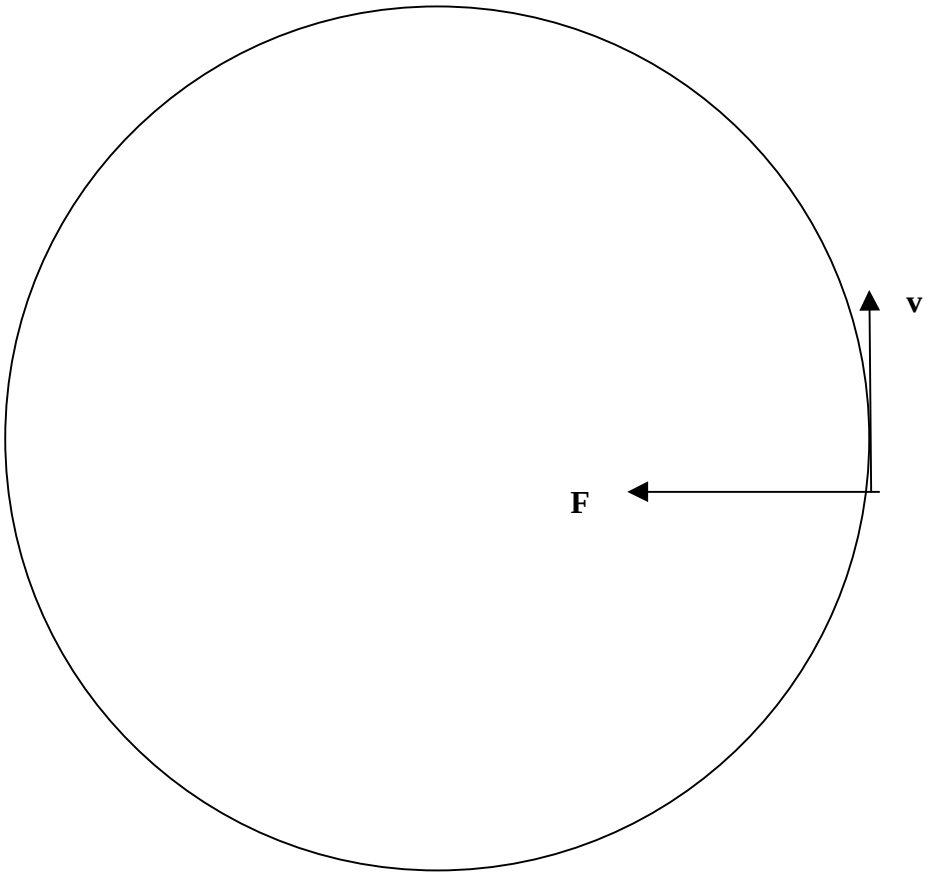

In order for there to be cyclotron motion, there has to be a force pushing in on the electron. This force is:

$$\mathbf{F} = -e\mathbf{v} \times \mathbf{B} \qquad \text{(I.8.1)}$$

This is the Lorentz Force Law for motion of electrons in a external magnetic field.

If the electrons move counterclockwise then the force points inward and one gets cyclotron motion. Note that protons would move clockwise. In the uniform uniaxial NMR magnetic field,

$\mathbf{B} = B_0\check{\mathbf{z}}$, so $F_{mag} = evB_0$. In order to get circular motion, the magnetic force has to be equal to the centrifugal force:

$$evB_0 = mv^2/r \qquad \text{(I.8.2)}$$

where r is the radius of the circular orbit and m is the electron mass. Using Eq. (I.4.9), we calculate that the angular frequency of the motion is:

$$\omega = v/r = (eB_0/m) \qquad \text{(I.8.3)}$$

Note that this is different by a factor of 2 than Eq.(1-25) in Harris. I believe that my calculation is correct. Let me know if you have found a mistake. The key thing is that the cyclotron frequency is independent of radius and velocity. Also, remember that $I = e\omega/2\pi$ so that the *induced current is proportional to B_0*.

So, we have a current loop. As discussed in Section 1-4, there is an associated magnetic moment μ. If you use equation I.4.7 and take into account the negative charge of the electron, you will see that the *induced electronic magnetic dipole moment* lies antiparallel to the external magnetic field direction. Because the induced moment is proportional to the induced current, the induced moment and its associated dipolar magnetic field are proportional to B_0. If the nucleus lies along the axis of cyclotron orbit, then the induced field will be antiparallel to the external field and hence reduce the field experienced by the nucleus. This effect is known as *chemical shielding*, where the chemical comes in because the magnitude of the shielding depends on the particular bonding (that is chemical) environment of the nucleus. So, the true field experienced by the nucleus is:

$$B = B_0(1-\sigma) \qquad \text{(I.8.4)}$$

where $\sigma << 1$. In diamagnetic molecules, (that is molecules with no unpaired electrons), σ is always positive. Typically, σ is quoted in ppm, that is parts per million. One multiplies the true σ by 10^6 to get ppm. For ^{1}H, the range of shieldings is about 10 ppm. For ^{13}C, it is about 200 ppm. The particular shielding depends of functional group. For example, the difference in average shielding for the ketone carbonyl C and methyl C is about 200 ppm.

In materials with unpaired electrons, the induced field from the unpaired electron can be significantly larger than that in diamagnetic materials. For example, in metalloproteins, the nuclei near the metal center(s), will be have significantly different shielding (and NMR frequencies) than the other nuclei. This effect allows one to determine which nuclei are close to the metal center. If the metal ion can be removed, the NMR spectra with and without the metal ion can be compared. In conductive materials, like metals, the induced conduction electron fields are parallel to the external field. This effect is called the *Knight Shift*. (see Slichter, Chapter 4.7) For example, the total magnetic field experienced by Cu is 0.23% (2300 ppm) greater in metallic copper than in $CuCl_2$.

Because the NMR frequency is linearly proportional to the magnetic field, the NMR frequency linearly decreases with increasing shielding. This frequency dependence is known as the *chemical shift*. Both shielding and shift are generally referenced to some reference compound for the particular nucleus, for example tetramethylsilane (TMS) for ^{13}C and ^{1}H, phosphoric acid

for ^{31}P, ammonium sulphate for ^{15}N. The shielding is quoted as $\sigma - \sigma_{ref}$ and the shift δ is quoted as:

$$\delta = (\nu - \nu_{ref})/\nu_{RF} = (\gamma/2\pi)B_0(\sigma_{ref}-\sigma)/\nu_{RF} \qquad \text{(I.8.5)}$$

Note that the shielding and shift go in opposite directions. As shielding increases, shift decreases. Increasing shift also means increasing NMR frequency. NMR spectra are typically displayed with shift and frequency increasing to the left. So, shielding increases to the right. There is another commonly used nomenclature: *upfield* and *downfield*. A nucleus shifted *downfield(upfield)* resonates with greater(lesser) chemical shift. This nomenclature is a historical artifact of the days of continuous wave NMR where the frequency was fixed and external magnetic field was swept. For resonance in this case,

$$\nu = (\gamma/2\pi)(B_0 + \Delta B)(1 - \sigma) \qquad \text{(I.8.6)}$$

In order to maintain the equality, when σ becomes smaller (greater), ΔB must also become smaller (greater). So smaller shielding and larger shifts correlate with smaller ΔB. This is downfield.

Shifts and shieldings are *anisotropic*, that is they depend on the orientation of the functional group of the nucleus relative to the external magnetic field direction. In liquids, the molecules tumble rapidly and NMR signals are only observed at the average chemical shift. In solids, the molecules are fixed in space and anisotropy is important. To understand this, let's consider a simple case of a C-H bond. We assume that the induced electronic dipole moment is antiparallel to the external field and at the center of the bond. Because of the angular nature of the dipolar field, the dipolar field will subtract (add) to the external field when the C-H bond is parallel (perpendicular) to the external field.

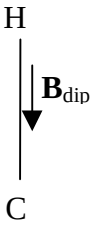

If we understand how the NMR frequency depends on functional group orientation relative to the external magnetic field direction (as can be measured from NMR on single crystals of model compounds where this orientation is known), then the solid state NMR spectrum contains a great deal of information. Each NMR frequency can be associated with a particular functional group orientation in the magnetic field. This information can be used in structural analysis, for example to determine the relative orientation of two functional groups in the molecule.

The range of chemical shift anisotropy for a particular nucleus can be large (for example about 200 ppm for ^{13}C in a C=O group) and in solid state spectra, gives one rather broad lines.

1.11 Spin-Spin Coupling

It is useful to compare various interactions:

Interaction	B_0 Dep.	Obs. in Liqs.	Obs. in Sols.	Orient.Dep.	Range ^{13}C (400 MHz)
Chemical Shift	Linear	yes	yes	no	20 kHz
Chemical Shift Anisotropy	Linear	no	yes	yes	20 kHz
Dipolar Coupling	None	no	yes	yes	7 kHz for dir. bonded ^{13}C
J(spin-spin) Scalar Coupling	None	yes	yes	no	50 Hz for dir. bonded ^{13}C, 150 Hz for ^{13}C-^{1}H, 1-10 Hz for ^{1}H-^{1}H separated by three Bonds

The energies of all the interactions are proportional to the $\gamma(\gamma s)$ of the nucleus (nuclei) involved.

The energy formula for the J-coupling between two spins 1 and 2 is:

$$U_J = hJ(I_{x1}I_{x2} + I_{y1}I_{y2} + I_{z1}I_{z2}) \qquad \text{(I.11.1)}$$

where the I_x, I_y, and I_z are the x, y, and z spatial components of nuclear spin angular momentum. Note that there are no vectors in this expression and hence no spatial or angular dependence. In most cases, we can neglect the $I_{x1}I_{x2} + I_{y1}I_{y2}$ term and only consider $JI_{z1}I_{z2}$. Despite its small size, J-coupling is observed in liquid state NMR because (1) the lines are sharp (~ 1 Hz linewidth) and (2) the larger dipolar couplings and chemical shift anisotropies (csa) are averaged out due to rapid molecular tumbling. In solids, the J-coupling is present but usually not apparent because of the much larger dipolar and csa interactions.

Numerical calculations of the J-coupling are difficult. This interaction is mediated through *bonds and bonding electrons* (See sections 8-17 through 8-26 in Harris). When the two nuclei are separated by more than three bonds, the J-coupling is generally negligible, less than 1 Hz. The *through-bond property* of J-coupling is different from the *through space* property of dipolar coupling (the two nuclei do not have to be connected through bonds). The actual formula for the classical dipolar coupling interaction between two nuclear magnetic moments μ_1 and μ_2 is (combine eqs. I.4.8 and I.5.1)

$$U_{dip} = (\mu_1 \cdot \mu_2)/r^3 - 3(\mu_1 \cdot \mathbf{r})(\mu_2 \cdot \mathbf{r})/r^5 \qquad \text{(I.11.2)}$$

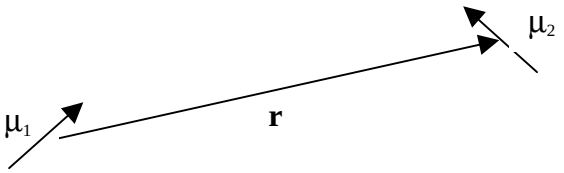

Note that the dipolar coupling depends on the relative orientation of the two spins as well as their orientation relative to the internuclear vector. A more sophisticated NMR analysis shows an additional dependence on the orientation of the internuclear vector relative to the external magnetic field direction.

So, the expression for the J-coupling is mathematically simpler than the dipolar coupling but it is more difficult to calculate the J-coupling magnitude.

The I's in Eq. (I.11.1) can be the same type of nucleus (homonuclear – e.g. ^{1}H, ^{1}H) or different types of nuclei (heteronuclear – e.g. ^{13}C – ^{1}H).

The analysis is similar in either case

Consider two spin ½ whose difference in NMR frequency is much larger than their J-coupling. Because of the small magnitude of the J-coupling, this case always holds in the heteronuclear J-coupling and usually holds for homonuclear J-coupling. We write the mathematical expression for this case as:

$$|\nu_1 - \nu_2| >> J \qquad \text{(I.11.3)}$$

where ν_1 and ν_2 are the NMR frequencies in the absence of J-coupling

Eq. I.11.3 may not hold when the two nuclei are chemically equivalent, for example the ^{1}H's in a methyl group. For this case, we will have do a different calculation.

When Eq. I.11.3 holds, we can neglect the $J(I_{x1}I_{x2} + I_{y1}I_{y2})$ energy term in Eq. (I.11.1) and only consider the $JI_{z1}I_{z2}$ term. We denote the individual spin states $m_I = +1/2$ and $m_I = -1/2$ as α and β, respectively. The coupled spin states will be: $\alpha_1\alpha_2$, $\alpha_1\beta_2$, $\beta_1\alpha_2$, $\beta_1\beta_2$. The chemical shift of nucleus 1 is δ_1, the chemical shift of nucleus 2 is δ_2, and their spin-spin coupling constant is J. The energy of a particular state is given by:

$$U = h[-\nu_{ref}(1 + \delta_1)m_{I1} - \nu_{ref}(1 + \delta_2)m_{I2} + Jm_{I2}m_{I2}] \qquad \text{(I.11.4)}$$

In NMR derivations, we typically neglect the h factor so that energy has units of frequency. Because of unit confusion, remember to distinguish *energy* from *transition frequency*. The minus sign in front of the ν_{ref} is true when we are dealing with a positive γ nucleus,e.g. ^{1}H (*cf.* Eq. I.5.2). Typically (although not always) δ_1, δ_2, and J are positive. We consider this specific case and draw the energy level diagram for two ^{1}H's under three different conditions: (a) *no* chemical shift and *no* J-coupling (b) chemical shift and *no* J-coupling and (c) chemical shift and J-coupling. In our example, $\delta_1 > \delta_2 > 0$. The NMR transitions which satisfy the single quantum selection rule are drawn in the figure.

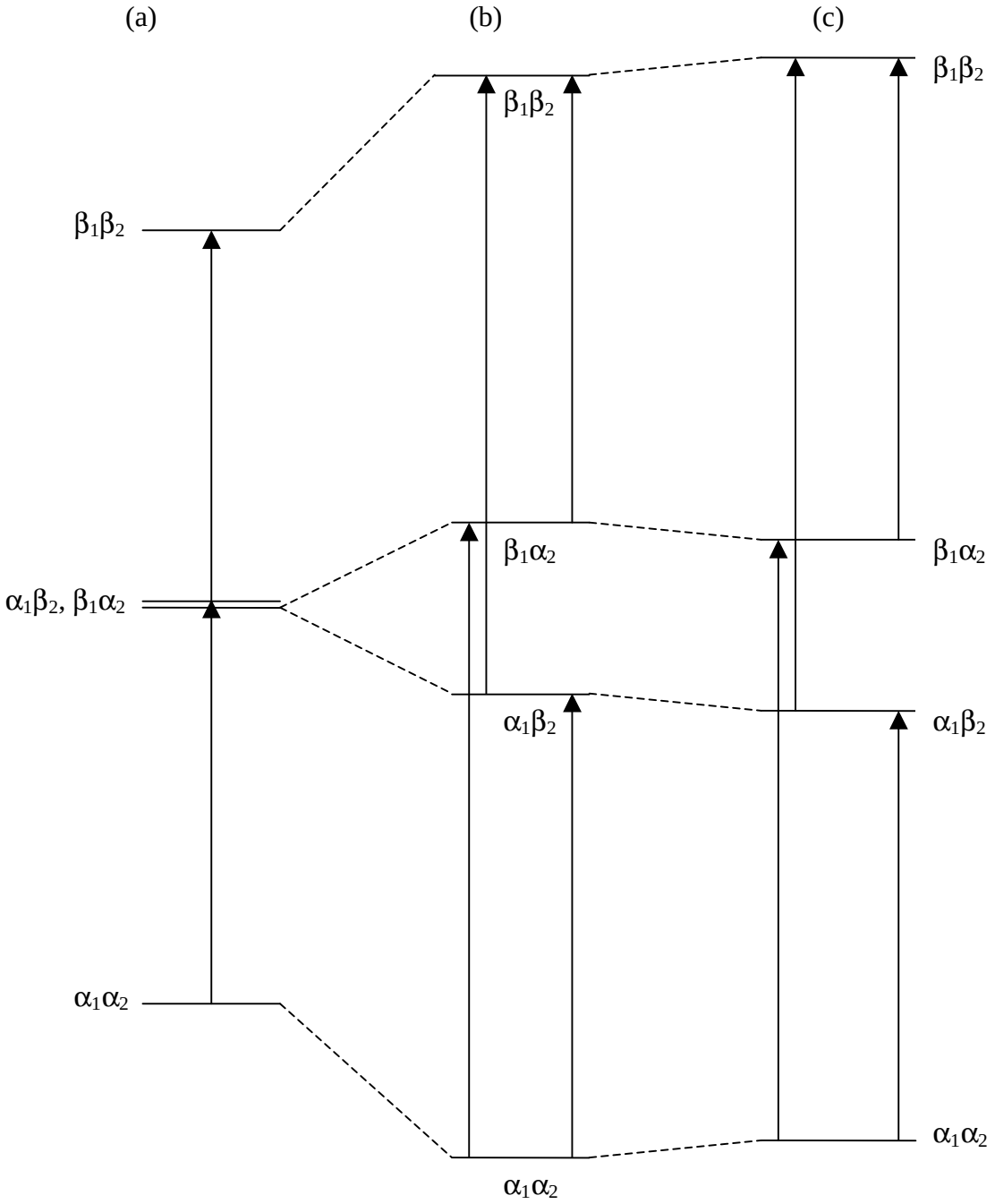

The NMR spectrum in the three cases is:

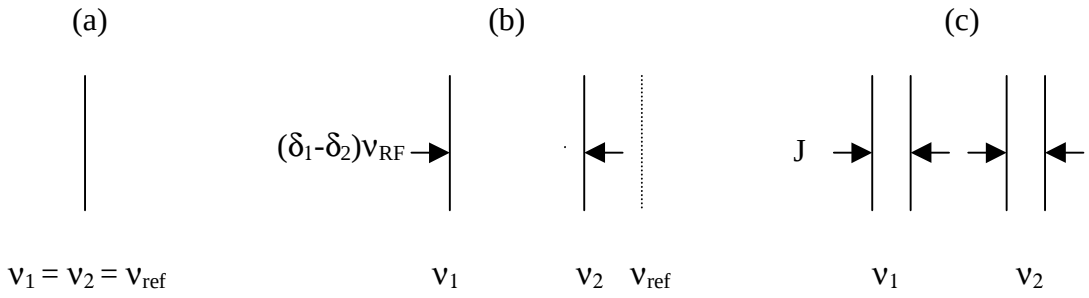

In the cases where Eq. (I.11.3) holds, additional spins can be added in a linear fashion.

Section 1.14 Equivalence

This is a somewhat confusing topic. We are trying to determine conditions for magnetic equivalence, that is the conditions when different nuclei have the same NMR spectrum. The general rule is this:

Two nuclei are magnetically equivalent when they are chemically equivalent <u>and</u> their couplings to all other nuclei in the molecule are the same.

This is a subtle point. Consider CH_2F_2 . Both ^1H and ^{19}F are spin ½ nuclei. *Because of the tetrahedral geometry*, the two ^1H are magnetically equivalent and the two ^{19}F are magnetically equivalent.

How does magnetic equivalence impact the NMR spectrum? In this case, the ^1H and ^{19}F NMR spectra are each composed of a triplet with intensities 1:2:1 and splitting equal to the ^1H-^{19}F J-coupling. Two questions are:

(1) Why are the ^1H-^1H and ^{19}F-^{19}F J-couplings not apparent in the spectra?
(2) Why does one observe this triplet?

We address the first question. We only consider the case of the two ^1H nuclei although equivalent arguments can be made for the two ^{19}F nuclei. In the absence of J-coupling, the two ^1H nuclei have the same NMR frequency, so Eq. (I.11.3) is not applicable. We have to do a different kind of analysis than what was described in Section 1.11.

When one has two or more equivalent particles, their states have to satisfy the Pauli Exclusion Principle, that is these states have to be either symmetric or antisymmetric with respect to particle exchange. In our two particle case, this means that exchanging the particle subscripts must give either the original state or –1 times the original state. The coupled states $\alpha_1\alpha_2$ and $\beta_1\beta_2$ are symmetric with respect to particle exchange. The states $\alpha_1\beta_2$ and $\beta_1\alpha_2$ are neither symmetric nor antisymmetric with respect to particle exchange. The physically correct states are the symmetric and antisymmetric linear combinations:

$(1/2)^{1/2}(\alpha_1\beta_2 + \beta_1\alpha_2)$	symmetric (S)	(I.11.5a)
$(1/2)^{1/2}(\alpha_1\beta_2 - \beta_1\alpha_2)$	antisymmetric (A)	(I.11.5b)

Transitions are forbidden between states with different spin symmetries so the antisymmetric state plays no part in the spectrum. In addition, Eq. (I.11.3) is not applicable and the energies of the states have to be calculated using the full J-coupling interaction $J(I_{x1}I_{x2} + I_{y1}I_{y2} + I_{z1}I_{z2})$. We show the energy diagram (a) in the absence of J-coupling and (b) in the presence of J-coupling. The allowed transitions are displayed.

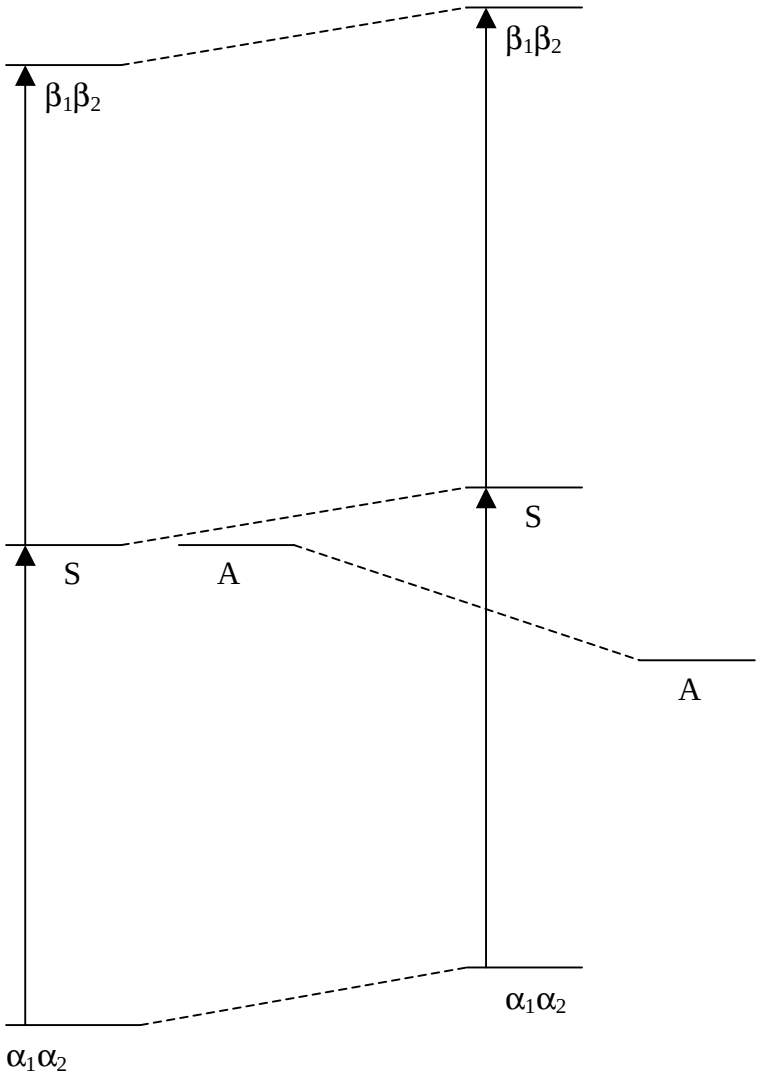

The J-coupling adds J/4 energy to each of the symmetric states and –3J/4 to the antisymmetric state. Because the NMR frequencies reflect the energy differences between the symmetric states, a single transition frequency is observed which is independent of the ^{1}H-^{1}H J-coupling.

We now address question (2), the observation of a 1:2:1 triplet with splitting equal to the ^{1}H-^{19}F J-coupling. This can be derived by considering the three spin system of ^{1}H coupled to two ^{19}F. We display the energy diagram and allowed transitions for (a) no coupling (b) one ^{1}H-^{19}F coupling (c) two ^{1}H-^{19}F couplings

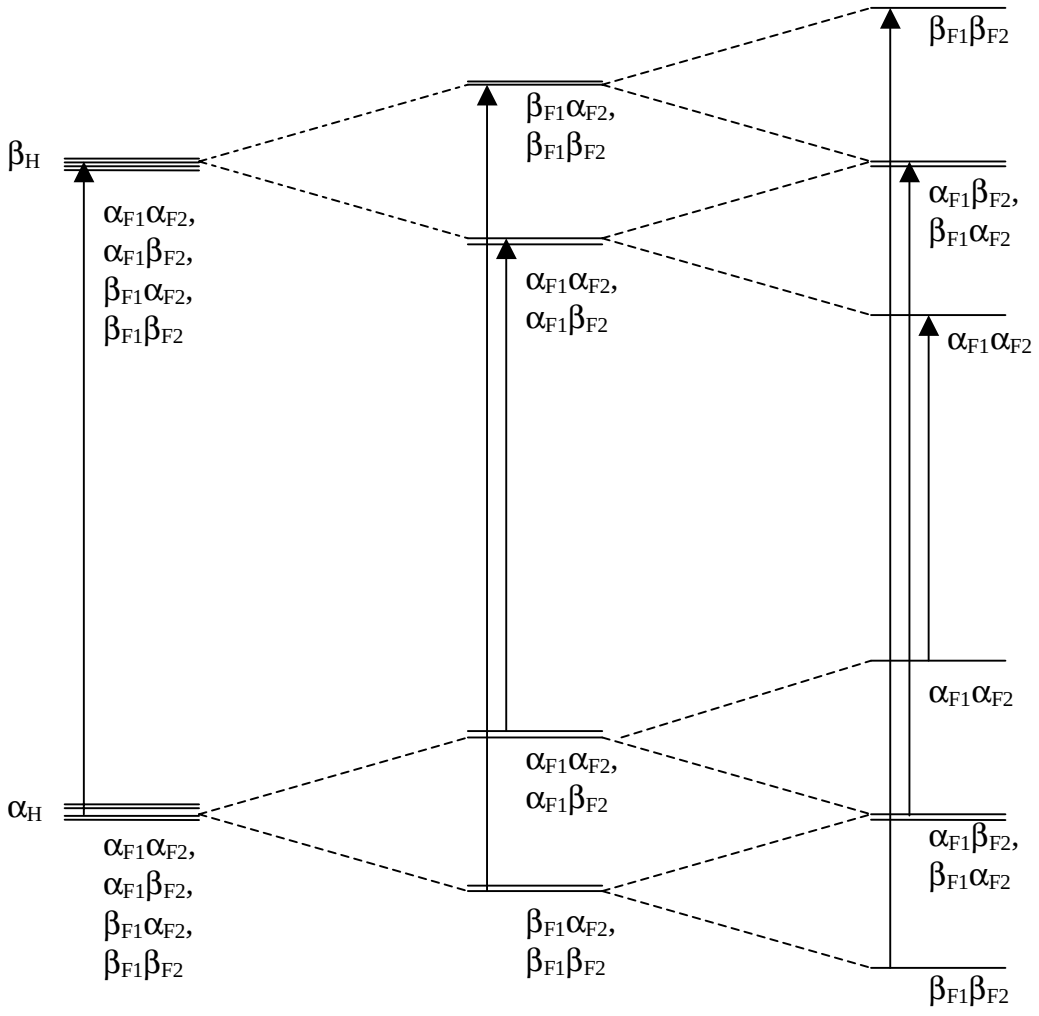

(a) (b) (c)

Remembering that only the ^{1}H changes its spin state in an NMR transition, the spectral frequency and 1:2:1 intensity pattern is clear from (c) in the energy diagram. For coupling to three ^{19}F, such as in CHF_3, the frequency splitting remains the same but the spectral pattern is composed of four lines with intensity ratio 1:3:3:1. In general, J-coupling to n equivalent spin ½ nuclei gives a pattern of n+1 lines separated by the J-coupling and in an intensity ratio given by Pascal's triangle.

Now consider the molecule 2,2-difluoroethylene:

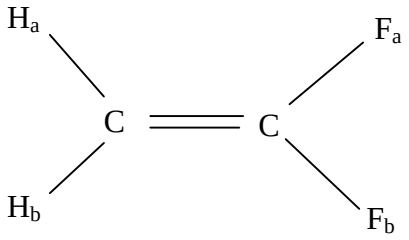

At first glance, you might think that the two ^{1}H are magnetically equivalent and the two ^{19}F are magnetically equivalent. However, neither pair satisfies the magnetic equivalence criterion. For example, the H_a-F_a J-coupling is through a cis-bond configuration while the H_b-F_a J-coupling is through a trans-bond configuration. The ^{1}H and ^{19}F NMR spectra are complicated (although understandable) as I showed you in class. The splitting frequencies can be used to derive all of the different kinds of J-couplings between the magnetically inequivalent nuclei.

Section 1-18: Decoupling

Decoupling is a means of eliminating splittings due to J- and dipolar couplings. It has the advantages of: (1) simplifying the NMR spectra and (2) improving signal-to-noise. For the second point, remember that the overall intensity of a transition is conserved so all of the intensity from the split signal is concentrated into the unsplit decoupled signal. One can apply either homo- or heteronuclear decoupling to eliminate homo- or hetero couplings. We concentrate on heteronuclear decoupling. A common application is decoupling of ^{13}C-^{1}H couplings while observing the ^{13}C signal. Experimentally, one applies an intense RF field at the ^{1}H Larmor frequency while detecting ^{13}C. Using a low-pass filter, one can suppress the ^{1}H RF in the ^{13}C detection electronics.

Why does decoupling work? We illustrate with a simple example of a single ^{13}C J-coupled to a single ^{1}H. In the undecoupled case (a), two transitions are observed separated by the ^{13}C-^{1}H J-coupling. In the decoupled case (b), a single transition is observed at the chemical shift of ^{13}C. With decoupling, the spectrum is the same as would be observed if there were no ^{1}H present in the material.

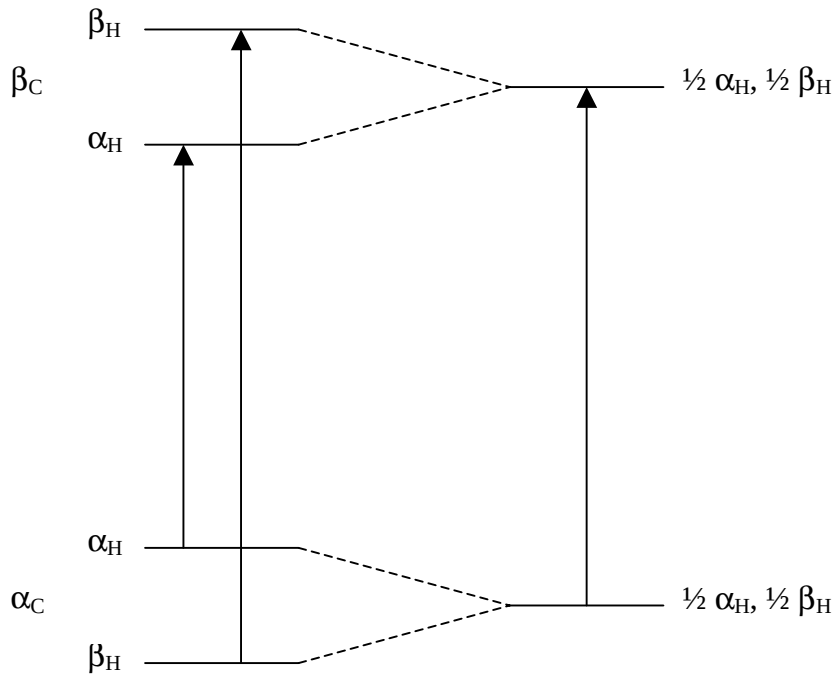

(a) (b)

With decoupling, the strong ^1H RF field induces transitions between the ^1H α and β spin states. The ^1H spin state is now a time-dependent linear combination of the α and β states:

$$\cos(\omega_R t/2)\alpha + i\sin(\omega_R t/2)\beta \qquad \text{(I.18.1)}$$

This is the *Rabi solution* whose derivation you can get from me or from many advanced quantum mechanics books. The ^1H oscillates between the α and the β states. The frequency of oscillation between these states is:

$$\nu_R = \omega_R/2\pi = \gamma_H B_1^H/h \qquad \text{(I.18.2)}$$

where B_1^H is the strength of the ^1H RF field. If

$$\nu_R >> J_{C\text{-}H} \qquad \text{(I.18.3)}$$

then the ^1H spin state seen by the ^{13}C is an average of α and β, that is m_H is effectively zero. Under this circumstance, the ^{13}C-^1H J-coupling interaction, $JI_{zC}I_{zH}$, will be zero.

The condition $\nu_R >> J_{C\text{-}H}$, is similar to the condition for motional narrowing in liquids. Whenever there is some process which interconverts states at a rate which is significantly faster than the energy (frequency) differences between these states, the ensemble of states is converted into a single 'average energy' state.

Rate Process	Interactions Averaged Out
Decoupling	J-coupling, dipolar coupling
Molecular Tumbling	Orientation-dependent interactions (e.g. csa, dipolar coupling, quadrupolar coupling)

In liquids, the molecular tumbling averages out the ^{13}C-^1H dipolar coupling so that the decoupling ν_R only has to be greater than $J_{C\text{-}H}$ which is ~ 150 Hz. In solids, ν_R has to be greater than the dipolar coupling $D_{C\text{-}H}$ which is > 30 kHz. Because the RF power is proportional to $(B_1^H)^2$, one needs orders of magnitude more powerful RF amplifiers and more robust probes to do solids NMR decoupling. In solids, a perennial problem is 'arcing', that is discharging in the NMR probe due to high RF power.

Section 1-20: Continuous-Wave NMR: the Spectrometer

Most of this section is cultural reading because very few people do CW NMR any more. One point which I would like to emphasize is 'shimming', which is ensuring that the external magnetic field is indeed uniform and uniaxial, $\mathbf{B} = B_0\mathbf{z}$. If the field is non-uniform, a range of NMR frequencies will be observed for a single transition, i.e. line-broadening. Line-broadening will degrade both resolution and sensitivity. In liquids, non-uniform fields can add significant line-broadening. In solids, the NMR signals are typically already broadened by an inherent inhomogeneous distribution of chemical shifts and non-uniformities in the magnetic field are much less apparent in the spectrum.

The main field in an NMR spectrometer is from the superconducting magnet, that is a set of coils which are superconducting at liquid He temperature. An additional set of room-temperature 'shim' coils surround the sample and are used to compensate for non-homogeneities in the superconducting field. The term 'shim' is an archaic one and dates back to where one would improve magnet homogenity by strategically placing thin pieces of metal (e.g. 'shims') in the magnet bore.

Each shim coil contributes a magnetic field with a particular spatial angular dependence. These are typically orders of spherical harmonics like the atomic orbitals (x,y,z,z^2, x^2-y^2, etc.) One typically varies the current (and hence magnetic field) from each of the coils to minimize the NMR linewidth. Because the effects of the shim coils are not orthogonal to one another, shimming is an iterative process. As an example, one type of field inhomogenity is:

$$B'_z\mathbf{z} \qquad \text{(I.20.1)}$$

In this case, the field is varying along the magnet axis so that different z positions in the sample experience different external magnetic fields. The z shim would be adjusted to provide a field $-B'_z\mathbf{z}$ to compensate for the inhomogeneity.

In addition, the superconducting field drifts with time. Usually, this drift is slow and uniform. On the 400 MHz NMR spectrometer, we just measured that this drift is about 9Hz/day at the ^{1}H frequency. If one has very sharp lines, as in liquids, and one signal averages for a long period of time, the magnet drift can also contribute to the linewidth. To compensate for the drift, there is a shim coil which provides a field $\Delta B\mathbf{z}$. The current in this coil is adjusted through a lock circuit which follows the drift of the ^{2}H signal in the sample. ^{2}H is used because liquid samples are usually dissolved in the deuterated solvents to minimize solvent ^{1}H background. The solvent ^{2}H provides a convenient large lock signal. ΔB is adjusted in time to keep a constant ^{2}H NMR frequency (*cf.* Eq. I.8.6) and hence external magnetic field.

Chapter 3: Relaxation and Fourier Transform NMR

Fourier transform NMR is used by most people today to obtain their NMR spectrum. We think about FT-NMR in a way which is different than most types of conventional spectroscopy.

Section 3-2: The Bloch Equations

One can think about NMR as a bulk phenomenom. We consider the net magnetic moment of the sample in a magnetic field. For simplicity, we consider a spin ½ nucleus. The magnetization **M** is simply the vector sum of the individual nuclear magnetic moments μ_i :

$$\mathbf{M} = \Sigma_i \mu_I \qquad \text{(III.2.1)}$$

The individual magnetic moments are the sum of three vector components:

$$\mu = \mu_x\mathbf{x} + \mu_u\mathbf{y} + \mu_z\mathbf{z} \qquad \text{(III.2.2)}$$

In an external magnetic field, only the μ_z component is quantized with definite values, either $+\gamma\hbar/2$ or $-\gamma\hbar/2$.

At thermal equilibrium, the components of transverse magnetization, M_x and M_y, will be 0 because the μ_x and μ_y values will be evenly distributed about zero and the sum of a large number of values from such a distribution is 0 (Show picture).

The thermal equilibrium value of the longitudinal magnetization M_z is not 0 because for positive γ, the spin up state has lower energy (and higher population) than the spin down state.

The value for M_z^{eq} can be calculated for N spin ½ nuclei as:

$$M_z^{eq} = M_0 = (N\gamma\hbar/2)[1 - \exp(-\gamma\hbar B_0/kT)]/[1 + \exp(-\gamma\hbar B_0/kT)] \approx N\gamma^2 B_0\hbar^2/4kT \qquad \text{(III.2.3)}$$

We can describe the time dependence of **M** in a magnetic field by using a generalization of Eq. (I.6.3). We simply sum the left and right-hand sides over all spins and can then substitute **M** for μ.

$$d\mathbf{M}/dt = -\gamma\mathbf{B} \times \mathbf{M} \qquad \text{(III.2.4)}$$

At thermal equilibrium **M** and **B** are parallel, so that there is no change in **M** with time (this is a definition of thermal equilibrium – no change in a macroscopic properties). At thermal equilibrium, **M** does *not* precess about the z (magnetic field) axis.

Suppose that **M** is at a non-thermal equilibrium value. Bloch postulated (correctly) that there are two characteristic times to return **M** to thermal equilibrium. T_2, the transverse or spin-spin relaxation time, is the characteristic time to return M_x and M_y to 0. T_1, the longitudinal or spin-lattice relaxation time, is the characteristic time to return M_z to M_0. Clearly $T_2 \leq T_1$. Longitudinal relaxation requires the change of spin state and through conservation of energy,

exchange of energy with lattice (phonon) modes. Transverse relaxation requires change of phase of the spin state and entails no energy exchange. For example,

a T_1 process: $\beta \rightarrow \alpha$
a T_2 process: $(2)^{1/2}(\alpha + \beta) \rightarrow (2)^{1/2}(\alpha - \beta)$

If the magnetic field is only the external magnetic field $B_0\mathbf{z}$, then the *Bloch equations* for time evolution of the magnetization are:

$$dM_x/dt = \gamma B_0 M_y - M_x/T_2$$

$$dM_y/dt = -\gamma B_0 M_x - M_y/T_2 \qquad \text{(III.2.5)}$$

$$dM_z/dt = -(M_z - M_0)/T_1$$

These are derived from Eq. (III.2.4) and inclusion of relaxation. Note that the transverse components M_x and M_y precess about the z axis with angular frequency γB_0, the nuclear Larmor frequency. In the presence of an RF field $(2B_1\cos\omega t)\mathbf{x}$, the Bloch equations are modified. As in Section 1.6, we decompose the linearly polarized radiation into a clockwise and counterclockwise component. Only the clockwise component is resonant with the positive-γ nuclei (which also rotate clockwise), and so the useful $\mathbf{B}_1$ RF field is:

$$\mathbf{B}_1 = (B_1\cos\omega t)\mathbf{x} - (B_1\sin\omega t)\mathbf{y} \qquad \text{(III.2.6)}$$

In the presence of this field, the Bloch equations are modified to:

$$dM_x/dt = \gamma[B_1\sin\omega t\, M_z + B_0 M_y] - M_x/T_2$$

$$dM_y/dt = -\gamma[B_0 M_x - B_1\cos\omega t\, M_z] - M_y/T_2 \qquad \text{(III.2.7)}$$

$$dM_z/dt = -\gamma[B_1\cos\omega t\, M_y + B_1\sin\omega t\, M_x] - (M_z - M_0)/T_1$$

As a kind of ‘foreshadowing’ to FT-NMR, we go into a frame which is rotating about the **z** axis at a frequency close to the Larmor frequency. Because there can actually be a distribution of Larmor frequencies because of different chemical shifts of different nuclei, we choose the RF frequency as our ‘rotating frame’ frequency. In this frame, a particular nuclear magnetic moment may precess slowly clockwise or counterclockwise because its Larmor frequency is slightly larger or smaller, respectively, than the RF frequency.

To describe the situation mathematically, we define new components of the transverse magnetization which rotate at the RF frequency and are perpendicular to one another.

$$u = M_x\cos\omega t - M_y\sin\omega t$$

$$v = M_x\sin\omega t + M_y\cos\omega t \qquad \text{(III.2.8)}$$

Note that $\omega = 2\pi\nu_{RF}$.

$$du/dt = dM_x/dt\ \cos\omega t - dM_y/dt\ \sin\omega t - \omega(M_x\ \sin\omega t + M_y\ \cos\omega t)$$
$$dv/dt = dM_x/dt\ \sin\omega t + dM_y/dt\ \cos\omega t + \omega(M_x\ \cos\omega t - M_y\ \sin\omega t) \qquad \text{(III.2.9)}$$

Using Eq. III.2.7 for dM_x/dt and dM_y/dt,

$$du/dt = \{\gamma[B_1 \sin\omega t\ M_z + B_0 M_y] - M_x/T_2\}\ \cos\omega t + \{\gamma[B_0 M_x - B_1 \cos\omega t\ M_z] - M_y/T_2\}\sin\omega t - \omega v$$

$$dv/dt = \{\gamma[B_1 \sin\omega t\ M_z + B_0 M_y] - M_x/T_2\}\ \sin\omega t - \{\gamma[B_0 M_x - B_1 \cos\omega t\ M_z] - M_y/T_2\}\cos\omega t + \omega u$$

Simplifying,

$$du/dt = \gamma B_0 v - u/T_2 - \omega v = (\omega_0 - \omega)v - u/T_2 = (\Delta\omega)v - u/T_2$$

$$dv/dt = -\gamma B_0 u + \gamma B_1 M_z - v/T_2 + \omega u = -(\omega_0 - \omega)u + \gamma B_1 M_z - v/T_2 = -(\Delta\omega)u + \gamma B_1 M_z - v/T_2$$

$$dM_z/dt = -\gamma B_1 v - (M_z - M_0)/T_1 \qquad \text{(III.2.10)}$$

The term $\Delta\omega$ is known as the resonance offset. Although we have written the rotating frame Bloch equations as having a single $\Delta\omega$, a real sample will have chemically different nuclei with different chemical shifts and hence different $\Delta\omega$. In a real calculation, it is necessary to take this range of chemical shifts into account.

$\Delta\omega$ can be thought of as a residual field which lies along the **z** axis. We can write Eqs. (III.2.10) in more familiar terms as:

$$d\mathbf{M}/dt = \mathbf{M}\ X\ (\gamma\mathbf{B}_1 + \Delta\omega\mathbf{z}) - (\mathbf{u} + \mathbf{v})/T_2 - (M_z - M_0)\mathbf{z}/T_1 \qquad \text{(III.2.11)}$$

where $\mathbf{M} = \mathbf{u} + \mathbf{v} + M_z\mathbf{z}$

Eqs. (III.2.10) are a special case of Eq. (III.2.11) where $\mathbf{B}_1 = B_1\check{\mathbf{u}}$. Eq. (III.2.11) is the rotating-frame equivalent of Eq. (III.2.4).

It is useful to understand the rotating frame Bloch equations under two limiting conditions.

(1) Strong B_1 fields: In this case, $\gamma B_1 >> \Delta\omega,\ 1/T_1,\ 1/T_2$.

$$du/dt = 0$$
$$dv/dt = \gamma B_1 M_z \qquad \text{(III.2.11)}$$

$$dM_z/dt = -\gamma B_1 v$$

The effect of the RF radiation is to rotate the magnetization in the vz plane in a counterclockwise direction as one looks out onto the u-axis. This is conventionally known as a pulse with minus x-phase. The x-phase is because the rotation is about the x-axis. The minus sign is by convention. In a modern NMR spectrometer, one can control the phase of the pulse in increments of less than a few degrees although the most common phases are +x,+y,-x,-y. (the 'quadrature phases'). What matters is the relative phase between the pulses. Once one denotes some RF phase as '+x', all other phases are defined relative to +x.

The angular rate of change of the magnetization is given by γB_1. It is often quoted in terms of the time to rotate the magnetization by $\pi/2$ (90 °) or by π (180 °). These times are known as *pulse lengths* and can be measured experimentally. Ideally the time required for a π pulse is twice the time for a $\pi/2$ pulse. In practice, this may not be the case, because it is not possible to turn the RF on instantaneously.

RF fields are also sometimes quoted as 'B_1 fields' which is in fact $\gamma B_1/2\pi$. One can interconvert between B_1 fields and pulse lengths by realizing that:

$$2\pi = (\omega_1)t_{2\pi} = (\gamma B_1)t_{2\pi}$$
$$\gamma B_1/2\pi = 1/t_{2\pi} \qquad \text{(III.2.12)}$$

So, the 'B_1 field' is just the inverse of the 2π pulse length. In pulsed FT-NMR, we apply a strong pulse of some length and create some (non-equilibrium) transverse magnetization. We then turn off the pulse (e.g. B_1 field).

(2) Then the rotating wave Bloch equations are:

$$du/dt = (\Delta\omega)v - u/T_2$$
$$dv/dt = -(\Delta\omega)u - v/T_2 \qquad \text{(III.2.13)}$$
$$dM_z/dt = -(M_z - M_0)/T_1$$

This case is known as "free induction". In NMR, we only detect the transverse magnetization and solve the u and v coupled differential equations. We define a new quantity

$$m = u + iv \qquad \text{(III.2.14)}$$

where i is the imaginary number. We can solve for m:

$$m(t) = m_0 e^{-i(\Delta\omega)t - t/T_2} \qquad \text{(III.2.15)}$$

where m_0 is the magnitude of the transverse magnetization at time t=0 (right after the RF is turned off). The two components of the transverse magnetization are:

$$u = m_0 \cos[(\Delta\omega)t] e^{-t/T_2}$$

$$v = -m_0 \sin[(\Delta\omega)t] e^{-t/T_2} \qquad \text{(III.2.16)}$$

These equations represent the time dependence of the rotating frame transverse magnetization in the absence of RF fields. This is the *free induction decay* (fid) which is measured in the NMR spectrometer. The two components are called the 'real' and 'imaginary' parts of the fid. Clearly, the two components oscillate sinusoidally in time and 90º out of phase with one another. They decay with the characteristic time T_2.

The NMR spectrum can be found from the Fourier Transform of the free induction decay m(t). The Fourier Transform is a mathematical transformation between the time and frequency domains:

$$F(\nu) = \int_{-\infty}^{+\infty} m(t) e^{2i\pi\nu t} dt \qquad \text{(III.2.17)}$$

(I have used a different sign convention than the book). The Fourier transform is symmetric so that:

$$m(t) = \int_{-\infty}^{+\infty} F(\nu) e^{-2i\pi\nu t} d\nu \qquad \text{(III.2.18)}$$

We can understand these equations easily in the absence of decay. In this case,

$$m(t) = m_0 e^{-i(\Delta\omega)t} \qquad \text{(III.2.19)}$$

$$F(\nu) = \int_{0}^{+\infty} m_0 e^{-i(\Delta\omega)t} e^{2i\pi\nu t} dt = \int_{0}^{+\infty} m_0 e^{-2i\pi(\Delta\nu)t} e^{2i\pi\nu t} dt = \int_{0}^{+\infty} m_0 e^{2i\pi(\nu - \Delta\nu)t} dt \qquad \text{(III.2.20)}$$

$$= m_0 \{ \int_{0}^{+\infty} \cos[2i\pi(\nu - \Delta\nu)t] dt + i \int_{0}^{+\infty} \sin[2i\pi(\nu - \Delta\nu)t] dt \} = m_0 \delta(\Delta\nu)$$

where $\delta(\Delta\nu)$ is the Dirac delta function. This function is only non-zero when $\nu = \Delta\nu$. (Note that the integral of a sine or cosine function over one period is zero unless its argument is 0.) So, $F(\nu)$ is only non-zero when $\nu = \Delta\nu$, that is the spectrum only has intensity at $\Delta\nu$ which is the resonance frequency of the nucleus (relative to the RF frequency) (Show picture).

The effect of relaxation is to give a distribution of frequencies about $\Delta\nu$ which have spectral intensity. For exponential decay of the fid, the Fourier Transform and spectral line profile is *Lorentzian*, which means it is proportional to:

$$[1/(T_2)]^2 / \{ 4\pi^2(\nu-\Delta\nu)^2 + [1/(T_2)]^2 \} \qquad \text{(III.2.21)}$$

The key to the linewidth is the denominator of Eq. (III.2.21). One can easily show that that the Full-Width at Half-maximum (FWHM) for the resonance is equal to $(1/\pi T_2)$. So as the relaxation rate increases, the decay of the FID increases and the spectrum broadens.

In the solid state, the linewidth may be inhomogeneous, that is it is dominated by a distribution of chemical shifts due to slightly different environments of the of the nucleus. The inhomogeneous lineshape is typically *gaussian* or statistical, that is proportional to:

$$\exp[-(\nu-\Delta\nu)^2/2\sigma^2] \qquad \text{(III.2.22)}$$

where σ is known as the *standard deviation*. The FWHM linewidth is: 2.35σ for a gaussian line. The Fourier Transform of a Gaussian is a Gaussian so a Gaussian lineshape will have a Gaussian FID and vice-versa.

III.8 Practical Fourier Transform NMR

We now have all of the background to understand pulsed Fourier Transform NMR. This is the kind of NMR which is done by nearly everyone and is the NMR used in this department:

First, a strong RF pulse is applied to create transverse magnetization. This is a non-equilibrium situation. The transverse magnetization precesses and decays to its equilibrium value of 0. This is recorded as the free induction decay. The Fourier Transform of the free induction decay is the NMR spectrum.

Why do we do Fourier Transform NMR? Up until the mid-1970's, almost everyone did continuous-wave (CW) NMR. This is ordinary spectroscopy, such as is done in a grating optical spectrometer. One scans the frequency and detects resonant absorption. Fourier Transform NMR has a great sensitivity advantage because the entire spectrum is obtained in a single acquisition (FID). One can signal-average easily by simply pulsing, acquiring an FID, waiting some delay period for recovery of longitudinal magnetization, and then pulsing and acquiring again, and so on. A second advantage is that pulsed NMR is much more amenable to sophisticated NMR than is CW NMR. By 'sophisticated', I mean multiple-pulse NMR which provides information other than the 1D NMR spectrum. This could be relaxation times, internuclear distances or torsion angles (molecular structure), or determination of nuclear connectivity (bonding).

(a) Spectrometer Block Diagram

I show a simplified diagram of a pulsed NMR spectrometer.

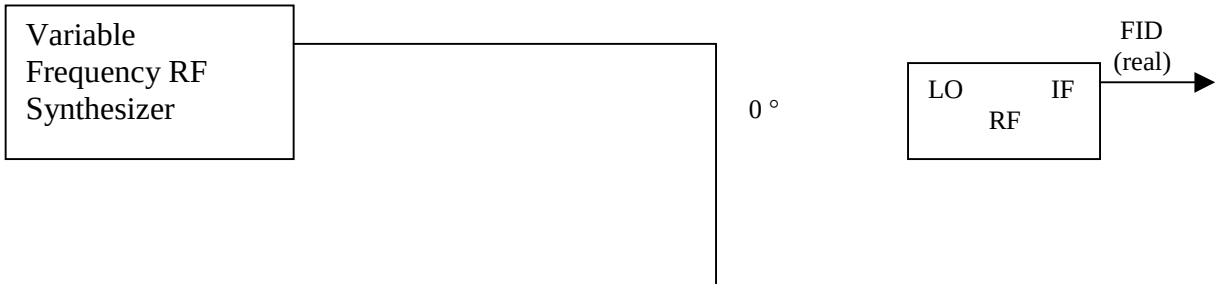

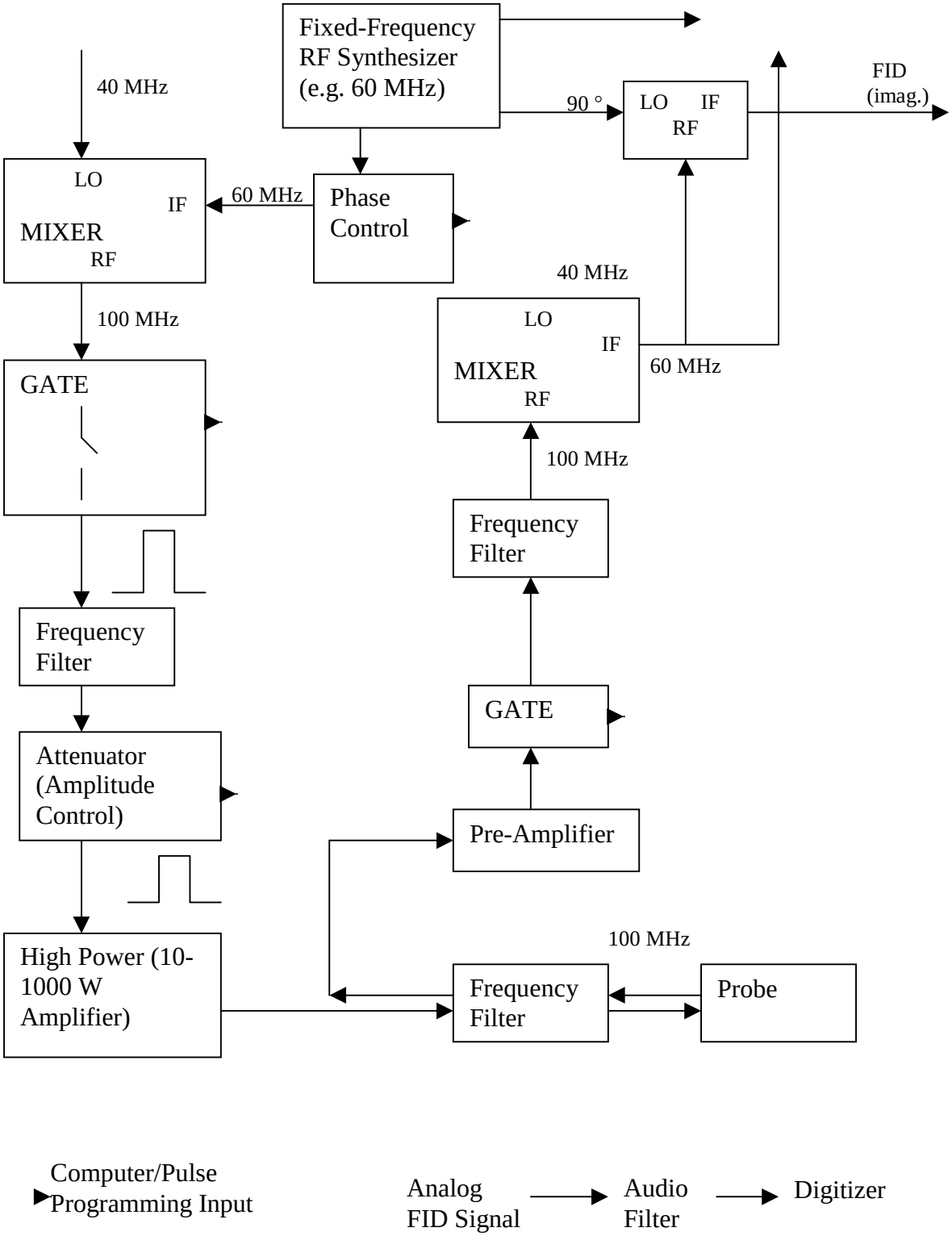

A Glossary of Terms:

Synthesizer: Puts out continuous RF wave at a particular frequency. This frequency may be fixed or can be variable and controllable.
Mixer: An rf device which takes the sum or difference of two frequencies. The three ports are RF, LO (local oscillator) and IF (intermediate frequency). In general, IF = RF ± LO . In general, two ports are used as inputs and one is an output. One obtains both the sum and difference frequencies and needs to use frequency filters to select just one of these frequencies. The output of the mixer is phase-sensitive to the inputs. For our purposes, an important point is that changing one of the input IF phase by 90° also changes the ouput RF phase by 90°.
Gate: Electronically Controlled Switch (TTL Digital Logic, +5 V ≡ on, 0 V ≡ off)
Attenuator: variable decreases RF amplitude (typically computer controllable e.g. 0.1 – 100% in 0.1% increments)
Amplifier: increases RF amplitude (and power) typically with fixed gain (e.g. x10) Remember that power is the square of amplitude. Amplitude is observed as voltage on an oscilloscope.
Frequency Filter: passes only certain frequencies, e.g. 100 MHz bandpass filter for passing ^{13}C frequencies, 400 MHz notch filter for blocking ^{1}H frequencies.

(a) Nature of the FID and Spectrum

Qualitative spectral information can be found by inspection of the FID. Each resonant frequency in the spectrum is found as an oscillation in the FID at the resonant (rotating frame) frequency $\Delta\nu$. Pi times the overall decay time constant of the FID gives approximately the inverse linewidth of the spectral transitions. For example, one can shim the system by adjusting the shim coil currents (1) to obtain minimal spectral linewidth or (2) to extend the FID for maximum time.

(b) Delay Times

Signal-to-noise can be improved by addition of FID's from multiple acquisitions. The delay time between acquisitions is limited by T_1, the characteristic time for longitudinal relaxation. If the system is not relaxed, then there is no longitudinal magnetization to be rotated into the transverse plane and hence no signal. The optimal signal-to-noise is determined by the pulse length, acquisition time, and T_1. In liquids, this can be:

$$\cos(\gamma B_1 t_{RF}) = \exp(-t_{ac}/T_1) \qquad \text{(III.8.1)}$$

where the cosine argument gives the pulse rotation angle and t_{ac} is the acquisition time.

In addition, one sometimes needs to worry about the *duty cycle*, the amount of time that the RF is on divided by the total period per acquisition (pulse time + acquisition time + delay time).

$$\text{duty cycle} = t_{RF}/(t_{RF} + t_{ac} + t_{delay}) \qquad \text{(III.8.2)}$$

In solids, the RF power is intense (hundreds of watts) and the duty cycle needs to be <5% to avoid heating the probe. Under these conditions, the optimal signal-to-noise is obtained using a $\pi/2$ pulse and $t_{delay} = 1.25T_1$.

(c) Excitation Bandwidth

The excitation bandwith is set by ~ $\pm 1/(2t_{RF})$ where t_{RF} is the amount of time the RF is on. This can be understood from the Fourier transform of a square pulse or from the (Heisenberg) Uncertainty Principle $(\delta\nu)(\delta t) \sim 1$. So, NMR spectra of samples with broader spectral widths require shorter pulses. This is particularly relevant for samples with large distributions of chemical shifts or in solids, samples with quadrupolar nuclei. In general, to observe a strong NMR signal, the magnetization typically should be rotated by an angle which is a significant fraction of $\pi/2$. If one shortens t_{RF}, one needs to increase the RF amplitude (B_1 field – cf. Eq. III.2.12) to maintain a constant rotation angle. Consequently, excitation of broader lineshapes requires shorter pulse times and greater RF power.

(d) Detection Bandwidth

The analog FID signal is digitized at discrete times. Digitization is required for computer fast fourier transform (FFT) and other spectral processing. The time increment between digitization is called the *dwell time*. A typical dwell time might be 20 μsec. The actual digitization time per point would be ~ 10 nsec. The detection bandwidth is $\pm 1/(2t_{dwell})$ around the RF frequency. This condition is set because detection of a particular frequency requires observation of two points per oscillation period. So, a dwell time of 20 μsec gives a total *sweepwidth* of 50 kHz. A broader spectrum requires a shorter dwell time. Because the detection bandwidth is inherently limited, low-pass audio filters are used prior to digitization to filter out higher-frequencies in the FID which will only contribute to spectral noise.

(e) Spectral Resolution

Spectral resolution can be limited by the *acquisition time = number of points X dwell time.* The linewidth associated with the acquisition time is ~ 1/(π X acquisition time). So, one wants to acquire for a time which is at least two times greater than the inherent decay time of the FID. An additional problem with too short acquisition times is a ringing pattern in the spectrum.

(f) Data Processing

Signal-to-noise can be improved by adding some additional decay to the FID. This can be either Gaussian or Lorentzian. Of course, this will broaden the spectral linewidths. The ‘smoothness’ of the spectrum can be improved by zero-filling the FID. This increases the number of points per unit frequency interval in the spectrum but does not improve spectral resolution. Baseline correction is usually used to improve the appearance of the spectrum and for improved quantitation of intensities. As the FID contains ‘real’ and imaginary components which are 90° out of phase with each other, the spectrum contains absorptive and dispersive components. Phasing is used to observe only purely absorptive spectra.

III.12 Measurement of T_1 by Inversion Recovery Method

We can measure the T_1's of nuclei in a sample with a simple pulse sequence 180°-τ-90°-FID-T_d where τ is varied and T_d is the delay time. Td should be much longer (5X) than T_1. The amount of longitudinal magnetization at the end of the τ period is:

$$M_z(\tau) = -2M_0\exp(-\tau/T_1) + M_0 = M_0[1 - 2\exp(-\tau/T_1)] \qquad \text{(III.12.1)}$$

For $\tau = 0$, $M_z(\tau) = -M_0$, and for $\tau = \infty$, $M_z(\tau) = +M_0$. At some intermediate time defined by $\tau_{null} = \ln 2 * T_1$, $M_z(\tau_{null})$ will be 0. The spectrum will follow the FID and go from emissive at short τ to absorptive at long τ. Different nuclei can have different T_1's. These are generally subtly different for chemically different ^{1}H's in organic liquids and solids but can be greatly different for chemically different heteronuclei (say aliphatic and carbonyl ^{13}C).

III.14 Spin-Echoes and the Measurement of T_2

Soon after the discovery of NMR, Hahn observed spin echoes, with which one can eliminate many kinds of loss of transverse magnetization including that due to chemical shift dispersion of a particular nucleus (like one finds in solids) and that due to magnetic field inhomogeneity. The basic spin echo sequence is 90°-τ-180°-τ-echo. Consider two nuclei, one which precesses faster than the RF and a second which precesses slower than the RF. During the first τ period, nucleus one will precess clockwise in the rotating frame and nucleus two will precess counterclockwise in the rotating frame. After the 180° pulse, the positions of nucleus one and two will be inverted. After the second τ period, the two nuclei will again be coincident in the rotating frame, hence the 'spin echo' or refocusing of transverse magnetization. The different precession frequencies could be due to a genuine chemical shift difference or because the magnetic field is inhomogeneous, that is not constant across the sample.

Genuine T_2 processes are not refocused in a spin echo. These processes can be thought of as arising from fluctuations in the Larmor frequencies of the nuclei. These fluctuations are not correlated either between nuclei or in time. T_2 can be measured from the decay of the echo with increasing n in the sequence 90°-[τ-180°-τ-echo]$_n$. Detection of the FID immediately after the echo followed by fourier transformation can be used to distinguish differences in T_2 between different nuclei.

III.15 The Theory of Relaxation

Relaxation theory is complicated and we will try to capture the spirit of it here. Any real problem requires mathematical and physical modeling. To understand relaxation, we must first understand that transitions between two states can be induced *radiatively* (that is by RF) or *non-radiatively* (no RF). Relaxation is concerned with non-radiative transitions.

The formal expressions for radiative and non-radiative transitions are similar. In both radiative and non-radiative cases for spin ½ nuclei, a transition is induced by interaction of the magnetic dipole with time-varying magnetic field. For radiative transitions, this is the RF field. For non-radiative transitions, this could be the dipolar field experienced by one nucleus due to a nearby nucleus. The dipolar field will be time-dependent because of molecular rotation or internuclear vibration. The transition rate will be proportional to:

$$W \sim |\gamma B'|^2 J(\omega) \qquad \text{(III.15.1)}$$

where B' is the fluctuating field strength and J(ω) (*the spectral density function*) is proportional tothe power available from this field at the appropriate angular transition frequency corresponding to the energy difference between the initial and final states. For example, for T_1 ($\beta \rightarrow \alpha$) type transitions, ω would be the 2π times the Larmor frequency whereas for T_2 ($\alpha\beta \rightarrow \beta\alpha$) type processes, there will be a contribution at zero frequency. If B' is the RF field, J(ω) would be one for $\beta \rightarrow \alpha$ transitions because all of the RF radiation oscillates at the Larmor transition frequency whereas for internal molecular fields J(ω) would be less than one because these fields oscillate at a range of frequencies relating to molecular motion.

J(ω) is the Fourier Transform of the auto-correlation function G(τ), the function which expresses the probability that the fluctuating field at time t+τ is the same as it was at time t. Typically, G(t) is a decaying exponential with *correlation time* τ_c.

$$G(\tau) = e^{-|\tau|/\tau c} \qquad \text{(III.15.2)}$$

The absolute value shows that correlation at times prior to t is equivalent to times after t. Recall that the Fourier Transform of an exponential is a Lorentzian giving

$$J(\omega) = 2\tau_c/(1 + \omega^2\tau_c) \qquad \text{(III.15.3)}$$

So, as the correlation time becomes shorter, there are more frequencies in the spectral density function (the Lorentzian becomes broader as its halfwidth occurs at $\omega=1/\tau_c$).

$(T_1)^{-1}$ is proportional to W giving

$$(T_1)^{-1} \sim |\gamma B'|^2\tau_c/(1 + \omega_0{}^2\tau_c) \qquad \text{(III.15.4)}$$

In general, τ_c is inversely proportional to rate of molecular motion, for example molecular tumbling or functional group reorientation. If $\omega_0{}^2\tau_c << 1$ (extreme narrowing), then

$$(1/T_1) \sim |\gamma B'|^2 \tau_c \qquad \text{(III.15.5)}$$

Increasing the temperature or decreasing viscosity will increase molecular tumbling, shorten τ_c, and give a *longer* T_1. In extreme narrowing, $T_2 \sim T_1$, of order 1 s in liquids. In solids extreme narrowing conditions do not hold and T_2 is typically in the μs-ms range while T_1 is in the seconds range. Equation III.5.4 gives a minimum $T_1 \sim \omega_0/|\gamma B'|^2$ when $\tau_c = (\omega_0)^{-1}$. As $\omega_0 \propto B_0$, the minimum T_1 increases with increasing external magnetic field.

Measurements of T_1 and T_2 for specific nuclei give information about the molecular motions specific to these nuclei (Show picture).

The fluctuating fields can be along the x, y, or z directions. To induce a T_1-type state-changing transition, the fluctuating field has to be transverse (like the RF field). The T_2-type fluctuating field can be either transverse or longitudinal. One typically measures T_2 starting with the magnetization fully aligned aligned (in the rotating frame) along one direction in the

transverse plane (e.g the 'y' direction). Only fields perpendicular to this direction (e.g. x,z) can cause T_2-type transitions or dephasing (*cf.* Eq. III.2.4).

III.16 Relaxation Mechanisms for Spin ½ Nuclei

There are a variety of relaxation mechanisms for spin ½ nuclei which have to do with different types of fluctuating magnetic fields. These include:

A. Dipole-Dipole Interaction with Other Nuclei: These interactions are modulated because of changes in the internuclear vector with time. The dipolar interaction depends as $(3\cos^2\theta-1)/r^3$ where θ is the angle between the internuclear vector and the external magnetic field and r is the internuclear distance. The dipolar interaction can be intramolecular or intermolecular and the magnetic field modulation can be due to molecular tumbling, functional group reorientation, vibration, or intermolecular translation. For ^{1}H relaxation in organic liquids and solids, dipolar fluctuations dominate the relaxation. Dipolar relaxation also dominates for heteronuclei with directly bonded ^{1}H.
B. Shielding: As a molecule or functional group moves relative to the external magnetic field, the shielding fields change because of the shielding anisotropy. This type of fluctuating field can dominate relaxation for heteronuclei with large shielding anisotropies and no directly bonded ^{1}H's such as non-aldehyde carbonyl carbons. Because the shielding is proportional to B_0, the shielding relaxation rate will be proportional to the square of the external field (Eq. III.15.1).
C. Interactions with Unpaired Electrons: Unpaired electrons interact with nuclei through both scalar and dipolar interactions. Because the electron dipole moment is three orders of magnitude larger than the nuclear dipole moment, these interactions can be significant. In room temperature liquids, the electron can change its spin state on the μsec timescale and in solids this rate can be significantly faster (and temperature-dependent). This change of spin state is one kind of modulation of the magnetic field. Also, in liquids, the motion of the paramagnetic species will modulate the nuclear-electron distances. It is sometimes convenient to add a paramagnetic reagent such as $Cr(acac)_3$ or $Cu(EDTA)_2$ to enhance nuclear spin relaxation times, particularly for heteronuclei in liquids or for frozen solution solids at low temperatures.

IV. Multi-Dimensional Pulsed NMR Spectroscopy (Chapter 7)

An important advantage of pulsed NMR spectroscopy is that one can add an arbitary number of *dimensions* or time periods during which one measures the FID or equivalently the NMR spectrum. One can then *correlate* the NMR spectra during these different time periods to obtain information about which nuclei are connected either through a few bonds or are nearby in space. These are the two pieces of information needed for determination of *molecular structure*.

There are many variants of multidimensional NMR spectroscopy. We consider the simplest pulse sequence to understand 2D NMR spectroscopy: $(90)_x$-t_1-$(90)_x$-t_2 . Consider a single spin with angular resonance offset $\Delta\omega$. After the first $\pi/2$ pulse, the transverse magnetization is:

$$m(0) = im_0 \qquad \text{(IV.1)}$$

where m_0 is the initial longitudinal magnetization. So, the magnetization lies initially along y axis. The magnetization precesses and decays (we assume exponentially) during the t_1 period and at the end of it:

$$\begin{aligned} m(t_1) &= im_0\exp(-i\Delta\omega t)\exp(-t_1/T_2) \\ &= m_0[\sin(\Delta\omega t_1) + i\cos(\Delta\omega t_1)]\exp(-t_1/T_2) \end{aligned} \qquad \text{(IV.2)}$$

The second $(90)_x$ pulse will have no effect on the real (x) component of transverse magnetization and rotate the imaginary (y) component to the -z axis. This gives:

$$m(t_1) = m_0[\sin(\Delta\omega t_1)]\ \exp(-t_1/T_2) \qquad \text{(IV.3)}$$

We detect the FID during t_2. This gives:

$$m(t_1,t_2) = m_0[\sin(\Delta\omega t_1)]\exp(-i\Delta\omega t_2)\exp(-t_1/T_2)\exp(-t_2/T_2) \qquad \text{(IV.4)}$$

We take the Fourier Transform with respect to t_2. This gives (*cf.* Section III.2):

$$F(t_1,\nu_2) = (m_0)^{1/2}[\sin(\Delta\omega t_1)]\exp(-t_1/T_2)\,S(\Delta\nu_2) \qquad \text{(IV.5)}$$

where $S(\Delta\nu_2)$ is a Lorentzian line of width $1/(\pi T_2)$ centered around the chemical shift $\Delta\nu$. The subscript is to label this frequency as being in the second dimension. $F(t_1,\nu_2)$ then is a Lorentzian line whose amplitude is determined by $m_0[\sin(\Delta\omega t_1)]$.

In 2D NMR spectroscopy, we take a series of t_2 FID's as a function of t_1. Following the t_2 Fourier Transformation, we then consider the t_1 FID's, that is we consider the signals as a series of t_1 FID's, each with a different ν_2 value. Using the pulse sequence described above, we only have the sine component of the t_1 FID in Eq. IV.5 . We obtain the cosine component with the sequence $(90)_x$-t_1-$(90)_{-y}$-t_2 . This will give after the $(90)_{-y}$ pulse:

$$m_{cos}(t_1) = m_0[i\cos(\Delta\omega t_1)]\exp(-t_1/T_2) \qquad \text{(IV.6)}$$

and after the t_2 period:

$$m_{cos}(t_1,t_2) = m_0[i\cos(\Delta\omega t_1)]\exp(-i\Delta\omega t_2)\exp(-t_1/T_2)\exp(-t_2/T_2) \quad \text{(IV.7)}$$

If we multiply Eqs. (IV.7) and (IV.4) by -i (equivalent to a 90 degree rotation of the transverse magnetization aka *phase shift*) and sum, we obtain:

$$m_{sum}(t_1,t_2) = m_0\exp(-i\Delta\omega t_1)\exp(-i\Delta\omega t_2)\exp(-t_1/T_2)\exp(-t_2/T_2) \quad \text{(IV.8)}$$

The FT with respect to t_2 gives:

$$F(t_1,\nu_2) = (m_0)^{1/2}\exp(-i\Delta\omega t_1)\exp(-t_1/T_2)\,S(\Delta\nu_2) \quad \text{(IV.9)}$$

The Fourier Transform with respect to t_1 is mathematically equivalent to that with respect to t_2 and yields:

$$F(\nu_1,\nu_2) = S(\Delta\nu_1)\,S(\Delta\nu_2) \quad \text{(IV.10)}$$

When we plot $F(\nu_1,\nu_2)$ as a 2D contour plot with $\nu_1$and ν_2 in each dimension, then we have a single 2D Lorentzian signal peaked at $\nu_1 = \nu_2 = \Delta\nu$.

This demonstrates 2D NMR spectroscopy but the result is trivial – the chemical shift is equivalent in each dimension.

2D spectroscopy becomes useful when we have additional interactions, for example scalar or dipolar coupling, or when we add some additional times which make the two dimensions inequivalent.

The multidimensional NMR experiment is divided up into preparation-(evolution-mixing)$_n$-detection. Each evolution-mixing period adds an additional dimension. In the sequence above, there is no mixing period. The preparation is the initial 90° pulse, the t_1 period is evolution, and the final 90° pulse and t_2 FID comprise detection.

The pulse sequence $(90)_x$-t_1-$(90)_x$-t_2 is the basis of the COSY (correlated spectroscopy) experiment in liquids. If one takes J-coupling into account, it can be shown that the COSY experiment gives crosspeaks between these J-coupled nuclei and is hence a means of determining which nuclei are connected by chemical bonds. By crosspeak, I mean a peak which has the NMR frequency of one nucleus in one dimension and the NMR frequency of a through-bond connected nucleus in the other dimension. The strength of the crosspeak is related to the strength of the J-coupling. More distant connectivities can be observed with the TOCSY pulse sequence.

The NOESY (Nuclear Overhauser Effect spectroscopy) pulse sequence is: $(90)_x$-t_1-$(90)_{x,y}$-t_{mix}-$(90)_x$-t_2 . With this sequence, one observes crosspeaks from nuclei which are near each other in space. In this sequence, there is a ‘mixing period’ of fixed time (typically ~ 100 ms) sandwiched

between the t_1 evolution and t_2 detection periods. During the mixing time, the stored longitudinal magnetization can undergo 'cross-relaxation' with nearby nuclei (<3-5 Å separation for ^{1}H) Cross-relaxation is mediated by dipolar (through-space) couplings between nearby nuclei. Cross-relaxation includes processes such as $\alpha_1\beta_2 \rightarrow \beta_1\alpha_2$ or $\alpha_1\alpha_2 \rightarrow \beta_1\beta_2$. The net effect is that magnetization which was on one nucleus during t_1 is on a nearby nucleus during t_2. After Fourier Transformation, this leads to crosspeaks which have the NMR frequency of one nucleus in the first dimension and the nearby nucleus in the second dimension. The intensity of a NOE crosspeak can be roughly correlated with internuclear distance ($\propto r^{-6}$). This distance dependence is derived from the r^{-3} dependence of the dipolar field and Eq. III.15.1. NOESY is the main sequence used for determination of molecular structure in liquids, particularly proteins.

The NOESY type sequence can also be used in solids. The rates of cross-relaxation are much faster in solids because of the much larger dipole couplings in solids. NOESY can be applied to low γ nuclei, such as nearby specifically labeled ^{13}C or ^{15}N. In addition to distance information derived from the crosspeak buildup rate as a function of τ_{mix}, relative orientation of functional groups can be derived from the dependence of crosspeak intensity on NMR frequency in each of the dimensions. Because the NMR frequency in solids depends in a well-known way on functional group orientation relative to the external magnetic field direction (CSA), the relative NMR frequencies of two nearby nuclei can be used to determine their relative functional group orientation.

There are several other kinds of 2D spectroscopy including heteronuclear correlation spectroscopy (HETCOR) for correlating the chemical shifts of directly bonded heteronuclei (for example, ^{15}N-^{1}H in proteins) and J-resolved spectroscopy for correlating the J-coupling with chemical shift for example ^{1}H-^{1}H coupling to ^{1}H chemical shift. Koji Nakanishi's book or Jeremy Evan's book on reserve in the chemistry library have good explanations and examples of 2D spectroscopies.

Resolution increases significantly with number of dimensions. You can understand this by considering the width of a single resonance $\delta\nu$ relative to the overall range of chemical shifts for a particular nucleus $\Delta\nu$. The number of chemically distinct nuclei which one can resolve in the 1D spectrum is $\sim \Delta\nu/\delta\nu = N$. In a 2D spectrum, the single resonance crosspeak area is $(\delta\nu)^2$ while the total chemical shift area is $(\Delta\nu)^2$. The number of distinct crosspeaks which one can resolve in the 2D spectrum is $\sim (\Delta\nu)^2/(\delta\nu)^2 = N^2$. So the number of resolvable peaks scales with the number of dimensions D like $(N)^D$. If there are N_1 magnetically distinct nuclei of a particular type (say ^{1}H) in the sample, then the actual number of off-diagonal crosspeaks will scale with dimension like $N_1(x)^{D-1}$ where x is the average number of neaby nuclei (perhaps 5-10 for ^{1}H in organic molecules). The resolving power should then increase as $N/N_1(N/x)^{D-1}$. N/x for ^{1}H's in liquids is ~ 100 and depends on linewidths and field strength This calculation is made by considering a 10 ppm dispersion in chemical shifts at 500 MHz field strength, 10 Hz linewidths, and x=5.

Extra dimensions decrease sensitivity because if one collects N_2 time points per dimension, then the amount of time per spectrum will scale as $(N_2)^D$. As in all spectroscopy, there is always a tradeoff between resolution and sensitivity.

V. A A Primer on Chemical Shift Anisotropy

The chemical shift anisotropy is the dependence of the chemical shift on the orientation of the functional group relative to the external magnetic field direction. The chemical shift anisotropy is governed by the chemical shift anisotropy principal values and three principal axes. Each axis is associated with a particular principal value (chemical shift). The principal axes are a 3D orthogonal axis system which is fixed relative to the functional group. For example, for ^{13}C in benzene, one axis is orthogonal to the plane and two are in the plane. For the amide (peptide) ^{13}C, one axis is perpendicular to the plane, one is approximately along the C=O bond and one is perpendicular to these other two.

The NMR chemical shift for a particular functional group orientation is governed by the equation:

$$\delta = \delta_{11} \cos^2\theta_{11} + \delta_{22} \cos^2\theta_{22} + \delta_{33} \cos^2\theta_{33} \qquad \text{(V.1)}$$

where δ_{11}, δ_{22}, and δ_{33} are the principal values and θ_{11}, θ_{22}, and θ_{33} are the angles between their respective principal axes and the external magnetic field direction. The cosine factors are called 'direction cosines'. Note that if the magnetic field is parallel to one of the principal axes, the chemical shift corresponds to its principal value.

Two of the principal axes correspond to functional group orientations which give the extrema of the possible chemical shifts. The third principal axis is perpendicular to the other two axes. The directions of the principal axes and their associated principal values can be governed by molecular symmetry and electronic environments. For benzene, the principal values are 10 ppm, 190 ppm, and 190 ppm. Note the molecular symmetry reflected in the principal values. For the amide group, the principal values are approximately 245 ppm, 185 ppm, and 90 ppm.

So, a particular functional group orientation corresponds to a particular chemical shift. In a single crystal, with a limited number of functional group orientations, the spectrum will be composed of several sharp lines. If one knows the orientations of the functional groups relative to the crystal axes and the orientation of the crystal axes relative to the external magnetic field direction, one can determine experimentally both the principal values and principal axes of the functional group. This determination is done by rotation of the crystal in the magnetic field and measurement of the changes in chemical shifts. The analysis is a solid geometry problem.

In a partially oriented system, there will be a range of observed chemical shifts. In an unoriented system, one observes the powder pattern characteristic of a system of fixed but randomly oriented functional groups. The two extrema and 'horn' in the powder pattern spectrum correspond to the three principal values. In Magic Angle Spinning spectra of unoriented samples, one can obtain the principal values from analysis of the relative intensities of the spinning sidebands as a function of spinning frequency.

In systems for which there is isotropic motion, such as liquids or high temperature solid C_{60}, one observes a chemical shift which is the average of shifts for all possible functional group orientations. This shift is calculated from:

$$\delta_{isotropic} = 1/3(\delta_{11} + \delta_{22} + \delta_{33}) \qquad \text{(V.2)}$$

V.B Resolution Enhancement in Multidimensional Experiments

This turns out to be more complicated than I initially thought. The improvement of resolution with increasing number of dimensions depends on the specific coupling pattern in the molecule. I treat one model example to give you some idea of the order of magnitudes involved. Consider some large molecule like a protein. We assume that each ^{1}H is coupled to two other nuclei, one ahead of it in the chain and one behind it. This is not a bad assumption for nuclear connectivities in a protein. For example, the 10^{th} ^{1}H is coupled to the 9^{th} and 11^{th} ^{1}H.

The 1D spectrum will be composed of 1000 signals spread over ~ 5000 Hz (for 10 ppm chemical shift dispersion at 500 MHz field strength). We define a dimensionless resolution parameter R:

$$R = (\text{Dispersion})/[(\text{Linewidth})(\#\ \text{Signals})] \qquad \text{(V.B.1)}$$

Spectral resolution should be proportional to R. For the 1D spectrum,

$$R(1D) = (5000\ \text{Hz})/[(10\ \text{Hz})(1000)] = 0.5 \qquad \text{(V.B.2)}$$

In the 2D case, the dispersion is $(5000\ \text{Hz})^2$ and the linewidth is $(10\ \text{Hz})^2$. In order to calculate the number of crosspeaks, we define a new notation for these peaks, (n_1,n_2), which means that we have the NMR frequency of nucleus n_1 in the first NMR dimension and the NMR frequency of nucleus n_2 in the second NMR dimension. For example, (10,11) would be the crosspeak between nucleus 10 in the first dimension and nucleus 11 in the second dimension. To calculate the number of crosspeaks in the 2D spectrum, we only consider cases where $n_1 \neq n_2$. This is reasonable because the $n_1=n_2$ cases are crowded along the 2D diagonal which takes up only $(2)^{1/2}(5000\ \text{Hz})(10\text{Hz}) \sim 70{,}000\ \text{Hz}^2$ of the $25{,}000{,}000\ \text{Hz}^2$ dispersion of the total 2D spectrum. Thus these diagonal peaks take up only ~0.3% of the total dispersion area and can be neglected in our resolution analysis. They provide no information about through-bond or through-space connectivity.

For each nucleus n_1 in the ν_1 dimension, there will be two off-diagonal crosspeaks in the 2D spectrum: $(n_1, n_1\text{-}1)$ and $(n_1, n_1\text{+}1)$; for example, (10,9) and (10,11). For 1000 distinct nuclei, there will be 2000 off-diagonal crosspeaks in the 2D spectrum. So,

$$R(2D) = (5000\ \text{Hz})^2/[(10\text{Hz})^2(2000)] = 125 \qquad \text{(V.B.3)}$$

So, the 2D spectrum has 250 times better resolution than the 1D spectrum.

In the 3D spectrum, we consider crosspeaks of the form (n_1,n_2,n_3). Again, we only consider the case where the three n are distinct. If all the n are all equal, they will lie along the body diagonal of the spectrum while if two are equal, they will lie along the diagonal of one of the 2D planes in the 3D spectrum.

For each nucleus n_1 in the ν_1 dimension, there will be two off-diagonal crosspeaks in the 3D spectrum, $(n_1, n_1\text{-}1, n_1\text{-}2)$ and $(n_1, n_1\text{+}1, n_1\text{+}2)$. So, there will be 2000 off-diagonal crosspeaks in the 3D spectrum. So,

$$R(3D) = (5000\ Hz)^3/[(10Hz)^3(2000)] = 62{,}500 \qquad \text{(V.B.4)}$$

For this particular coupling case, you can easily show that the number of off-diagonal crosspeaks is independent of the number of dimensions for two dimensions or higher, so the resolution improves as (5000 Hz/10 Hz) = 500 with each additional dimension.

VI. Quantum Mechanics of Spins

A. Homonuclear Coupled Spin System

The Hamiltonian for two spin ½ A and B in a liquid is the sum of the chemical shift and the J-coupling term:

$$H = -\nu_0 (1 + \delta_A) I_{Az} - \nu_0 (1 + \delta_B) I_{Bz} + J(\mathbf{I}_A \cdot \mathbf{I}_B) \qquad \text{(VI.A.1)}$$

$$= -\nu_0 (1 + \delta_A) I_{Az} - \nu_0 (1 + \delta_B) I_{Bz} + J(I_{Ax} I_{Bx} + I_{Ay} I_{By} + I_{Az} I_{Bz})$$

$$= -\nu_0 (1 + \delta_A) I_{Az} - \nu_0 (1 + \delta_B) I_{Bz} + J(I_{Az} I_{Bz}) + J/2(I_{A+} I_{B-} + I_{A-} I_{B+})$$

We now solve for the energy eigenvalues and eigenstates of the coupled spin Hamiltonian.

We consider the Schrodinger Equation:

$$H |\psi\rangle = E |\psi\rangle \qquad \text{(VI.A.2)}$$

We consider a state which is the linear combination of our four product states.

$$|\psi\rangle = c_{\alpha\alpha}|\alpha\alpha\rangle + c_{\alpha\beta}|\alpha\beta\rangle + c_{\beta\alpha}|\beta\alpha\rangle + c_{\beta\beta}|\beta\beta\rangle \qquad \text{(VI.A.3)}$$

We wish to solve for the energies and sets of coefficients which satisfy the Schrodinger Equation.

$$\begin{aligned} H |\psi\rangle = {} & \{-\nu_0 [1 + (\delta_A + \delta_B)/2] + J/4\} c_{\alpha\alpha} |\alpha\alpha\rangle \\ & + \{\nu_0 (\delta_B - \delta_A)/2] - J/4\} c_{\alpha\beta} |\alpha\beta\rangle + (J/2)\, c_{\alpha\beta} |\beta\alpha\rangle \\ & + \{\nu_0 (\delta_A - \delta_B)/2] - J/4\} c_{\beta\alpha} |\beta\alpha\rangle + (J/2)\, c_{\beta\alpha} |\alpha\beta\rangle \\ & + \{\nu_0 [1 + (\delta_A + \delta_B)/2] + J/4\} c_{\beta\beta} |\beta\beta\rangle \\ = {} & E (c_{\alpha\alpha}|\alpha\alpha\rangle + c_{\alpha\beta}|\alpha\beta\rangle + c_{\beta\alpha}|\alpha\beta\rangle + c_{\beta\beta}|\beta\beta\rangle) \end{aligned} \qquad \text{(VI.A.4)}$$

We now create four equations by projecting $\langle\alpha\alpha|$, $\langle\alpha\beta|$, $\langle\beta\alpha|$, and $\langle\beta\beta|$ onto both sides of Eq. (VI.A.4). We take advantage of the orthonormality of these spin functions.

$$\{-\nu_0[1 + (\delta_A + \delta_B)/2] + J/4\}c_{\alpha\alpha} = E\, c_{\alpha\alpha}$$

$$\{\nu_0(\delta_B - \delta_A)/2] - J/4\}c_{\alpha\beta} + (J/2)c_{\beta\alpha} = E\, c_{\alpha\beta}$$

$$(J/2)\, c_{\alpha\beta} + \{\nu_0(\delta_A - \delta_B)/2] - J/4\}c_{\beta\alpha} = E\, c_{\beta\alpha} \qquad \text{(VI.A.5)}$$

$$\{\nu_0[1 + (\delta_A + \delta_B)/2] + J/4\}c_{\beta\beta} = E\, c_{\beta\beta}$$

We bring the E terms over to the left hand side of the equation.

$$\{-\nu_0[1 + (\delta_A + \delta_B)/2] + J/4 - E\}c_{\alpha\alpha} = 0$$

$$\{\nu_0(\delta_B - \delta_A)/2] - J/4 - E\}c_{\alpha\beta} + (J/2)c_{\beta\alpha} = 0$$

$$(J/2)\, c_{\alpha\beta} + \{\nu_0(\delta_A - \delta_B)/2] - J/4 - E\}c_{\beta\alpha} = 0 \qquad \text{(VI.A.6)}$$

$$\{\nu_0[1 + (\delta_A + \delta_B)/2] + J/4 - E\}c_{\beta\beta} = 0$$

We can write this in matrix form as Eq. VI.A.7:

$$\begin{matrix} \{-\nu_0[1 + (\delta_A + \delta_B)/2] + J/4 - E\} & 0 & 0 & 0 \\ 0 & \{\nu_0(\delta_B - \delta_A)/2] - J/4 - E\} & J/2 & 0 \\ 0 & J/2 & \{\nu_0(\delta_A - \delta_B)/2] - J/4 - E\} & 0 \\ 0 & 0 & 0 & \{\nu_0[1 + (\delta_A + \delta_B)/2] + J/4 - E\} \end{matrix} \begin{matrix} c_{\alpha\alpha} \\ c_{\beta\alpha} \\ c_{\beta\alpha} \\ c_{\beta\beta} \end{matrix} = 0$$

We wish to solve this matrix equation for values of E and the coefficients. This is a linear algebra problem. We first solve for E. There is a theorem from linear algebra which says that the values of E which satisfy this equation are those for which the *determinant* of the matrix is 0.

How do we calculate the determinant of this matrix? The determinant of a 2 x 2 matrix is:

$$\begin{matrix} c_{11} & c_{12} \\ c_{21} & c_{22} \end{matrix} = c_{11}c_{22} - c_{21}c_{12} \qquad \text{(VI.A.8)}$$

The determinant of a 3 x 3 matrix is:

$$\begin{vmatrix} c_{11} & c_{12} & c_{13} \\ c_{21} & c_{22} & c_{23} \\ c_{31} & c_{32} & c_{33} \end{vmatrix} = c_{11}\begin{vmatrix} c_{22} & c_{23} \\ c_{32} & c_{33} \end{vmatrix} - c_{12}\begin{vmatrix} c_{21} & c_{23} \\ c_{31} & c_{33} \end{vmatrix} + c_{13}\begin{vmatrix} c_{21} & c_{22} \\ c_{31} & c_{32} \end{vmatrix} \qquad \text{(VI.A.9)}$$

The determinant of a 4 x 4 matrix is the sum of four 3 x 3 determinants and so forth.

In our case, the determinant equation is:

$$\{-\nu_0[1 + (\delta_A + \delta_B)/2] + J/4 - E\} \times \{\nu_0[1 + (\delta_A + \delta_B)/2] + J/4 - E\}$$

$$\times \det \begin{vmatrix} \{\nu_0(\delta_B - \delta_A)/2] - J/4 - E\} & J/2 \\ J/2 & \{\nu_0(\delta_A - \delta_B)/2] - J/4 - E\} \end{vmatrix} = 0 \qquad \text{(VI.A.10)}$$

Clearly,

$$E = -\nu_0[1 + (\delta_A + \delta_B)/2] + J/4$$

and (VI.A.11)

$$E = \nu_0[1 + (\delta_A + \delta_B)/2] + J/4$$

are eigenvalue solutions to the determinant equation for the $|\alpha\alpha\rangle$ and $|\beta\beta\rangle$ eigenfunctions, respectively.

The other solutions are the solutions to the equation:

$$\det \begin{vmatrix} -\Delta - J/4 - E & J/2 \\ J/2 & \Delta - J/4 - E \end{vmatrix} = 0 \qquad \text{(VI.A.12)}$$

where $\Delta = \nu_0(\delta_A - \delta_B)/2$.

The solutions are:

$$E = (1/4)\{-J \pm 2(J^2 + 4\Delta^2)^{1/2}\} \qquad \text{(VI.A.13)}$$

In the extreme that $\Delta >> J$, $E \approx \pm \Delta/2$ with eigenfunctions $|\alpha\alpha\rangle$ and $|\beta\beta\rangle$. This is the heteronuclear case, for example Δ = 150,000,000 Hz (for ^{13}C, ^{1}H on a 400 MHz system) and J=150 Hz (directly bonded).

In the extreme that $\Delta = 0$ (magnetically equivalent nuclei), E = -3J/4 and J/4. In this case, we can solve for the set of coefficients $c_{\alpha\beta}$ and $c_{\beta\alpha}$ for each value of E by plugging it into the Equations (VI.A.7). We also include the normalization condition.

$$E = -3J/4 \Rightarrow (1/2)^{-1/2} (|\alpha\beta\rangle - |\beta\alpha\rangle)$$
$$E = J/4 \Rightarrow (1/2)^{-1/2} (|\alpha\beta\rangle + |\beta\alpha\rangle) \qquad \text{(VI.A.14)}$$

Harris gives the solution for the intermediate case in terms of J and $D = (J^2 + 4\Delta^2)^{1/2}$.

The total NMR intensity for the coupled spin system is always a constant but the individual intensities vary with J/Δ. As Δ approaches 0 (magnetic equivalence), we go from four transitions to a single transition. This is the derivation of why we do not observe J-coupling in magnetically equivalent systems.

VI.B Density Matrix

In Section VI.A, I introduced the matrix approach to quantum mechanics. For example, Eq. VI.A.7 is the matrix equivalent of the equation:

$$(H\text{-}E)|\psi\rangle = 0 \qquad \text{(VI.B.1)}$$

The matrix element of an operator A in the jth row and kth column is $\langle\phi_j| A |\phi_k\rangle$ where the ϕ_j and ϕ_k are the *basis* functions. For a single spin ½, these basis functions would be $|\alpha\rangle$ and $|\beta\rangle$. For two spin ½, these could be the product functions $|\alpha\alpha\rangle$, $|\alpha\beta\rangle$, $|\beta\alpha\rangle$, and $|\beta\beta\rangle$.

For example, in the Section VI.A. example, the second row, third column element of the Hamiltonian matrix is $\langle\alpha\beta| H |\beta\alpha\rangle = J/2$.

For a single spin ½, you can easily calculate that the spin operators have matrices:

$$I_x = \tfrac{1}{2}\begin{matrix} 0 & 1 \\ 1 & 0 \end{matrix} \qquad I_y = \tfrac{1}{2}\begin{matrix} 0 & -i \\ i & 0 \end{matrix} \qquad I_z = \tfrac{1}{2}\begin{matrix} 1 & 0 \\ 0 & -1 \end{matrix}$$

$$I_+ = \begin{matrix} 0 & 1 \\ 0 & 0 \end{matrix} \qquad I_- = \begin{matrix} 0 & 0 \\ 1 & 0 \end{matrix} \qquad \text{(VI.B.2)}$$

I have reversed the order from Harris, p. 44. In pulsed NMR experiments, an important operator is the density operator:

$$\rho(t) = |\psi(t)\rangle \langle\psi(t)| \qquad \text{(VI.B.3)}$$

where $\psi(t)$ is the total spin wavefunction at time t. One also considers the density matrix of the density operator. Consider for example, a single spin ½ with wavefunction:

$$|\psi(t)\rangle = c_\alpha(t)|\alpha\rangle + c_\beta(t)|\beta\rangle \qquad \text{(VI.B.4)}$$

Its density matrix will be:

$$\rho(t) = \begin{matrix} c_\alpha(t)\, c_\alpha^*(t) & c_\alpha(t)\, c_\beta^*(t) \\ c_\beta(t)\, c_\alpha^*(t) & c_\beta(t)\, c_\beta^*(t) \end{matrix} \qquad \text{(VI.B.5)}$$

One other important point about the total density matrix is that it is actually the *sum* of matrices VI.B.5 for all molecules in the sample. For those of you who've had statistical mechanics, it is the *ensemble average*. We will treat this averaging in a simple way.

The on-diagonal density matrix elements give you the *populations* of individual basis states while the off-diagonal elements give you *coherences* between states.

You can show that the average value for some observable *A* is the *trace* of the product matrix between the *A* operator matrix and the density matrix. The *trace* is the sum of the diagonal elements of the matrix:

$$\langle A\rangle(t) = \mathrm{Trace}(A\rho(t)) \qquad \text{(VI.B.6)}$$

For example, consider that the wavefunction at time τ for all spins is given by equal mixtures of $|\alpha\rangle$ and $|\beta\rangle$:

$$|\psi(\tau)\rangle = (2)^{-1/2}\,|\alpha\rangle + (2)^{-1/2}|\beta\rangle \qquad \text{(VI.B.7)}$$

The density matrix is:

$$\rho(\tau) = \tfrac{1}{2}\begin{matrix} 1 & 1 \\ 1 & 1 \end{matrix} \qquad \text{(VI.B.8)}$$

You can easily show that $\langle I_x\rangle(\tau) = \tfrac{1}{2}$, $\langle I_y\rangle(\tau) = 0$, $\langle I_z\rangle(\tau) = 0$.

If instead

$$|\psi(\tau)\rangle = (2)^{-1/2}\,|\alpha\rangle + i(2)^{-1/2}|\beta\rangle \qquad \text{(VI.B.9)}$$

then

$$\rho(\tau) = \tfrac{1}{2}\begin{matrix} 1 & -i \\ i & 1 \end{matrix} \qquad \text{(VI.B.10)}$$

and

$$\langle I_x\rangle(\tau) = 0,\ \langle I_y\rangle(\tau) = \tfrac{1}{2},\ \langle I_z\rangle(\tau) = 0.$$

These calculations are important because in an NMR experiment, we detect the transverse magnetization $M_x + iM_y$ which is proportional to $\gamma\hbar(I_x + iI_y) = \gamma\hbar I_+$. Using the density matrix approach, we can then calculate the observable magnetization. Only those parts of the density matrix which depend only on I_x or I_y contribute to the observable magnetization. These are the *single quantum coherence* terms in the density matrix. You can partly understand this because $\mathrm{Tr}(I_x^2) = \mathrm{Tr}(I_y^2) = \tfrac{1}{2}$.

The time-dependent Schrodinger Equation can be calculated in terms of the density matrix. We calculate the time evolution of the density matrix under the pulse sequence and then use this

density matrix calculation to calculate the observable transverse magnetization during the detection period.

VI.C Time Evolution of the Density Matrix and the Product Operator Formalism

Two forms of the time-dependent Schrodinger Equation are:

$$d\rho/dt = (i/\hbar)(\rho H - H\rho) \qquad \text{(VI.C.1)}$$

and

$$\rho(t) = e^{-(i/\hbar)Ht}\,\rho(0)\,e^{(i/\hbar)Ht} = U_H(t)\,\rho(0)\,U_H^{-1}(t) \qquad \text{(VI.C.2)}$$

where $U_H(t) = e^{-(i/\hbar)Ht}$ is known as the *propagator*. From Eq. (VI.C.1), we see that the time evolution of the density matrix at time t is governed by those parts of the density matrix which do not commute with the Hamiltonian at time t.

In a typical NMR sequence, we start at thermal equilibrium. For a system of single spin ½ at thermal equilibrium, the density matrix has no off-diagonal elements and the on-diagonal elements represent the thermal populations of the $|\alpha\rangle$ and $|\beta\rangle$ states.

$$\rho(0) = \begin{matrix} c_\alpha(0)\,c_\alpha^*(0) & 0 \\ 0 & c_\beta(0)\,c_\beta^*(0) \end{matrix} = \begin{matrix} 1 + \hbar\omega/2kT & 0 \\ 0 & 1 - \hbar\omega/2kT \end{matrix}$$

$$= \tfrac{1}{2}\begin{matrix} 1 & 0 \\ 0 & 1 \end{matrix} + (\hbar\omega/2kT)(\tfrac{1}{2})\begin{matrix} 1 & 0 \\ 0 & -1 \end{matrix} \qquad \text{(VI.C.3)}$$

The first term is the identity operator and commutes with everything. It makes no contribution to the evolution of the density matrix nor to the observed FID. The second term is equal to $(\hbar\omega/2kT)I_z$. You can easily show using Eq. (VI.B.6) and Eq. (VI.C.3) that at thermal equilibrium $\langle I_x\rangle = 0$, $\langle I_y\rangle = 0$, and $\langle I_z\rangle = (\hbar\omega/4kT)$. At thermal equilibrium, there is no transverse magnetization and the longitudinal magnetization for n spins will be:

$$\langle M_z\rangle = n\gamma\hbar\langle I_z\rangle = n\gamma^2\hbar^2 B_0/4kT \qquad \text{(VI.C.4)}$$

This is the Curie Law.

We consider a spin system of two like spin ½ , for example two ^{1}H. The interesting part of the thermal equilibrium density matrix will be:

$$\rho(0) = (\hbar\omega/2kT)\,(I_{z1} + I_{z2}) \qquad \text{(VI.C.5)}$$

In liquid state NMR, the molecular Hamiltonian for two spins in the weak J-coupling limit is:

$$H = (-\hbar\omega_1)I_{z1} - (\hbar\omega_2)I_{z2} + (2\pi\hbar J)I_{z1}I_{z2} \qquad \text{(VI.C.6)}$$

The ω_1 and ω_2 are sum of the Zeeman and chemical shift angular frequencies for nucleus 1 and nucleus 2, respectively. In the weak coupling limit, we have neglected the terms $2\pi\hbar J(I_{x1}I_{x2} + I_{y1}I_{y2})$. With this kind of simple Hamiltonian and RF pulses, the time propagation of the density matrix can be understood in terms of *product operators*.

At all times, the density matrix will just be the sum of products of nuclear spin operators.

In the density matrix propagation, the RF pulses act as rotations on the nuclear spin operators. For example, a pulse of phase x with rotation angle θ acts on different nuclear spin components in the density matrix as follows:

$$e^{i\theta I_{x1}} I_{x1} e^{-i\theta I_{x1}} = I_{x1}$$

$$e^{i\theta I_{x1}} I_{y1} e^{-i\theta I_{x1}} = I_{y1}\cos\theta - I_{z1}\sin\theta \qquad \text{(VI.C.7)}$$

$$e^{i\theta I_{x1}} I_{z1} e^{-i\theta I_{x1}} = I_{z1}\cos\theta + I_{y1}\sin\theta$$

Note that the rotations follow the right-hand rule for $d\mathbf{I}/dt = \gamma\mathbf{I} \times \mathbf{B}$.

We can also use expressions such as Eq. (VI.C.7) to calculate the time propagation of the density matrix under the Zeeman and chemical shift (first two terms) of the molecular Hamiltonian. The effect of the J-coupling is described by (see Slichter, Section 7.26):

$$e^{-i\theta I_{z1}I_{z2}} I_{x1} e^{i\theta I_{z1}I_{z2}} = I_{x1}\cos(\theta/2) + 2I_{y1}I_{z2}\sin(\theta/2)$$

$$e^{-i\theta I_{z1}I_{z2}} I_{y1} e^{i\theta I_{z1}I_{z2}} = I_{y1}\cos(\theta/2) - 2I_{x1}I_{z2}\sin(\theta/2) \qquad \text{(VI.C.8)}$$

$$e^{-i\theta I_{z1}I_{z2}} I_{z1} e^{i\theta I_{z1}I_{z2}} = I_{z1}$$

In our case $\theta = 2\pi Jt$, *cf*. Eqs. (VI.C.2), (VI.C.6). Note that under the influence of J-coupling, the density matrix can oscillate between single spin and two spin terms. This oscillation is very important for COSY and other pulse sequences.

VI.D COSY Pulse Sequence

We use the density matrix and product operators to understand the basic COSY pulse sequence: $(\pi/2)_x$-t_1-$(\pi/2)_x$-t_2 .

The interesting part of the equilibrium density matrix is given by Eq. (VI.C.5). We only consider the propagation of one of the spin operators I_{z1} . The propagation of I_{z2} will be the same except all of the 1 and 2 subscripts will be interchanged in the expressions.

The density matrix $\rho(t_1,t_2)$ is proportional to:

$$\rho(t_1,t_2) = e^{it_2(\omega_1 I_{z1} + \omega_2 I_{z2} - 2\pi J\, I_{z1}I_{z2})}\, e^{(i\pi/2)(I_{x1}+ I_{x2})}\, e^{it_1(\omega_1 I_{z1} + \omega_2 I_{z2} - 2\pi J\, I_{z1}I_{z2})}\, e^{(i\pi/2)(I_{x1}+ I_{x2})}\, I_{z1}$$
$$e^{-(i\pi/2)(I_{x1}+ I_{x2})}\, e^{-it_1(\omega_1 I_{z1} + \omega_2 I_{z2} - 2\pi J\, I_{z1}I_{z2})}\, e^{-(i\pi/2)(I_{x1}+ I_{x2})}\, e^{-it_2(\omega_1 I_{z1} + \omega_2 I_{z2} - 2\pi J\, I_{z1}I_{z2})} \qquad \text{(VI.D.1)}$$

You can see that time increases from I_{z1} in the center outwards.

We calculate the density matrix systematically from the center out. The first $\pi/2$ pulse:

$$e^{(i\pi/2)(I_{x1}+ I_{x2})}\, I_{z1} e^{-(i\pi/2)(I_{x1}+ I_{x2})} = e^{(i\pi/2)(I_{x1})}\, e^{(i\pi/2)(I_{x2})} I_{z1} e^{-(i\pi/2)(I_{x2})}\, e^{-(i\pi/2)(I_{x1})}$$
$$= e^{(i\pi/2)(I_{x1})}\, I_{z1}\, e^{-(i\pi/2)(I_{x1})} = I_{y1} \qquad \text{(VI.D.2)}$$

The second step can only be done when the individual terms in the exponential argument commute with one another. The third step results from the fact that an operator on spin 2 has no effect on spin 1. The fourth step uses the third equation in Eq. (VI.C.7).

Now we calculate the propagation of the density matrix during the t_1 period . All of the terms in the molecular Hamiltonian commute with one another.

$$e^{it_1(-2\pi J\, I_{z1}I_{z2} + \omega_1 I_{z1} + \omega_2 I_{z2})}\, I_{y1}\, e^{-it_1(\omega_2 I_{z2} + \omega_1 I_{z1} - 2\pi J\, I_{z1}I_{z2})}$$
$$= e^{it_1(-2\pi J\, I_{z1}I_{z2})}\, e^{it_1(\omega_1 I_{z1})}\, e^{it_1(\omega_2 I_{z2})}\, I_{y1}\, e^{-it_1(\omega_2 I_{z2})}\, e^{-it_1(\omega_1 I_{z1})}\, e^{-it_1(-2\pi J\, I_{z1}I_{z2})}$$
$$= e^{it_1(-2\pi J\, I_{z1}I_{z2})}\, e^{it_1(\omega_1 I_{z1})}\, I_{y1}\, e^{-it_1(\omega_1 I_{z1})}\, e^{-it_1(-2\pi J\, I_{z1}I_{z2})} \qquad \text{(VI.D.3)}$$
$$= e^{it_1(-2\pi J\, I_{z1}I_{z2})}\, \{I_{y1}\cos(\omega_1 t_1) + I_{x1}\sin(\omega_1 t_1)\} e^{-it_1(-2\pi J\, I_{z1}I_{z2})}$$
$$= I_{y1}\cos(\omega_1 t_1)\cos(\pi J t_1) - 2I_{x1}I_{z2}\cos(\omega_1 t_1)\sin(\pi J t_1) + I_{x1}\sin(\omega_1 t_1)\cos(\pi J t_1)$$
$$+ 2I_{y1}I_{z2}\sin(\omega_1 t_1)\sin(\pi J t_1)$$

We calculate the effect of the second $(\pi/2)_x$ pulse.

$$e^{(i\pi/2)(I_{x1})}\, e^{(i\pi/2)(I_{x2})}\{\, I_{y1}\cos(\omega_1 t_1)\cos(\pi J t_1) - 2I_{x1}I_{z2}\cos(\omega_1 t_1)\sin(\pi J t_1) + I_{x1}\sin(\omega_1 t_1)\cos(\pi J t_1)$$
$$+ 2I_{y1}I_{z2}\sin(\omega_1 t_1)\sin(\pi J t_1)\,\}\, e^{-(i\pi/2)(I_{x1})}\, e^{-(i\pi/2)(I_{x2})}$$
$$= -I_{z1}\cos(\omega_1 t_1)\cos(\pi J t_1) - 2I_{x1}I_{y2}\cos(\omega_1 t_1)\sin(\pi J t_1) + I_{x1}\sin(\omega_1 t_1)\cos(\pi J t_1)$$
$$- 2I_{z1}I_{y2}\sin(\omega_1 t_1)\sin(\pi J t_1) \qquad \text{(VI.D.4)}$$

We are now ready to look at the evolution in t_2. This is actually the time when we detect the FID which is proportional to $\mathrm{Tr}\{(I_{1+} + I_{2+})\rho(t_1,t_2)\}$. This will only be non-zero for those parts of $\rho(t_1,t_2)$ which contain only I_{1-} or I_{2-} . For our purposes, this means the interesting part of $\rho(t_1,t_2)$ is those terms which contain a single operator I_{x1}, I_{y1}, I_{x2}, or I_{y2} .

With this in mind, we can neglect the first term in Eq. (VI.D.4) because it contains I_{z1} and will not evolve under the molecular Hamiltonian propagator. We can also neglect the second term which will always contain a product of operators. We first calculate the t_2 propagation of the third term:

$$e^{it_2(-2\pi J I_{z1}I_{z2})}\, e^{it_2(\omega_1 I_{z1})}\, e^{it_2(\omega_2 I_{z2})}\, \{ I_{x1}\sin(\omega_1 t_1)\cos(\pi J t_1) \}$$

$$e^{-it_2(\omega_2 I_{z2})}\, e^{-it_2(\omega_1 I_{z1})}\, e^{-it_2(-2\pi J I_{z1}I_{z2})}$$

$$= e^{it_2(-2\pi J I_{z1}I_{z2})}\, \{[\sin(\omega_1 t_1)\cos(\pi J t_1)]\,[I_{x1}\cos(\omega_1 t_2) - I_{y1}\sin(\omega_1 t_2)]\}\, e^{-it_2(-2\pi J I_{z1}I_{z2})}$$

$$\approx [\sin(\omega_1 t_1)\cos(\pi J t_1)]\,[I_{x1}\cos(\omega_1 t_2)\cos(\pi J t_2) - I_{y1}\sin(\omega_1 t_2)\cos(\pi J t_2)] \qquad \text{(VI.D.5)}$$

In the last step, I have neglected the two spin term because it does not contribute to the FID experimental signal. For $\omega_1 >> \pi J$, which is always true, one can show that the density matrix oscillates at angular frequencies $\omega_1 \pm \pi J$ in each dimension. These frequencies will also be found in the calculated FID and give rise to four diagonal peaks in the 2D spectrum at real frequencies $(\nu_{\text{first dimension}}, \nu_{\text{second dimension}}) = (\nu_1 \pm J/2, \nu_1 \pm J/2)$. In each dimension there will be two peaks separated by J.

Now we consider the t_2 evolution of the fourth term in Eq. (VI.D.4)

$$e^{it_2(-2\pi J I_{z1}I_{z2})}\, e^{it_2(\omega_1 I_{z1})}\, e^{it_2(\omega_2 I_{z2})}\, \{-2I_{z1}I_{y2}\sin(\omega_1 t_1)\sin(\pi J t_1)\}$$

$$e^{-it_2(\omega_2 I_{z2})}\, e^{-it_2(\omega_1 I_{z1})}\, e^{-it_2(-2\pi J I_{z1}I_{z2})}$$

$$= e^{it_2(-2\pi J I_{z1}I_{z2})}\, \{[\sin(\omega_1 t_1)\sin(\pi J t_1)][-2I_{z1}I_{y2}\cos(\omega_2 t_2) - 2I_{z1}I_{x2}\sin(\omega_2 t_2)]\, e^{-it_2(-2\pi J I_{z1}I_{z2})}$$

$$\approx [\sin(\omega_1 t_1)\sin(\pi J t_1)]\,[\, I_{x2}\cos(\omega_2 t_2)\sin(\pi J t_2) - I_{y2}\sin(\omega_2 t_2)\sin(\pi J t_2)\,] \qquad \text{(VI.D.6)}$$

In the last step, I used Eq.(VI.C.8) but neglected the two-spin terms which do not contribute to the FID experimental signal. Eq. (VI.D.6) gives rise to signals in the density matrix which oscillate at angular frequencies $\omega_1 \pm \pi J$ in t_1 and $\omega_2 \pm \pi J$ in t_2. After Fourier transformation of the calculated two-dimensional FID, these oscillations give rise to four *crosspeaks* with real frequencies $(\nu_{\text{first dimension}}, \nu_{\text{second dimension}}) = (\nu_1 \pm J/2, \nu_2 \pm J/2)$. The four peaks are not all in phase with one another.

If you look back through these equations, you see that the crosspeaks arise from development of two spin density matrix terms in t_1 which are rotated by the second $\pi/2$ pulse and then evolve back into single spin (observable) terms in t_2. The transfer of magnetization from single spin 1 to

two-spin coherence to single spin 2 is governed by the *J-coupling*. In other words, the J-coupling mediates transfer of magnetization from spin 1 in the first NMR dimension to spin 2 in the second NMR dimension. This is why one only observes *through-bond connectivity* in COSY. If J = 0, then Eq. VI.D.6 equals 0.

The product operator approach to the density matrix is fundamental to understanding complex liquid state NMR pulse sequences. In solid state NMR, the dipole couplings are typically strong, that is the $I_{x1}I_{x2} + I_{y1}I_{y2}$ contributions are non-negligible, and the product operator approach is not useful. For solid state NMR sequences, the density matrix is numerically propagated in matrix form. *Average Hamiltonian theory* is also useful for understanding the spectra obtained with solid state NMR sequences.